JCI The Journal of Clinical Investigation

TRPV4 channel opening mediates pressure-induced pancreatitis initiated by Piezo1 activation

Sandip M. Swain, … , Steven R. Vigna, Rodger A. Liddle

J Clin Invest. 2020. https://doi.org/10.1172/JCI134111.

Research In-Press Preview Gastroenterology

Graphical abstract

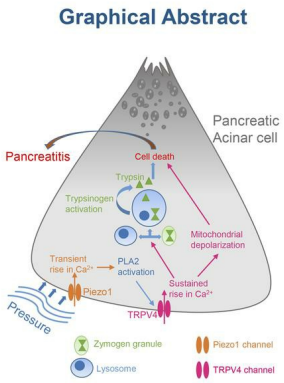

TRPV4 channel opening mediates pressure-induced pancreatitis initiated by Piezo1 activation

Sandip M. Swain[1], Joelle M. -J. Romac[1], Rafiq A. Shahid[1], Stephen J. Pandol[5], Wolfgang Liedtke[3], Steven R. Vigna[1,2], Rodger A. Liddle[1,4]

Departments of Medicine[1], Cell Biology[2], and Neurology[3], Duke University and Department of Veterans Affairs Health Care System[4], Durham, North Carolina 27710 and Cedars Sinai Medical Center[5], Los Angeles, California

Address correspondence to:

Rodger A. Liddle, M.D.
Box 103859
1033A Genome Science Research Building 1
905 LaSalle Street
Duke University Medical Center
Durham, NC 27710

Telephone: (919) 681-6380
Email: rodger.liddle@duke.edu

Keywords: Transient receptor potential vanilloid subfamily 4, shear stress, mitochondrial depolarization, trypsinogen activation, pancreatitis, mechanoreceptor, phospholipase A2

Conflict of interest: The authors have declared that no conflict of interest exists.

Abstract

Elevated pressure in the pancreatic gland is the central cause of pancreatitis following abdominal trauma, surgery, endoscopic retrograde cholangiopancreatography (ERCP), and gallstones. In the pancreas excessive intracellular calcium causes mitochondrial dysfunction, premature zymogen activation, and necrosis ultimately leading to pancreatitis. Although stimulation of the mechanically activated, calcium-permeable ion channel, Piezo1, in the pancreatic acinar cell is the initial step in pressure-induced pancreatitis, activation of Piezo1 produces only transient elevation in intracellular calcium that is insufficient to cause pancreatitis. Therefore, how pressure produces a prolonged calcium elevation necessary to induce pancreatitis is unknown. We demonstrate that Piezo1 activation in pancreatic acinar cells caused a prolonged elevation in intracellular calcium levels, mitochondrial depolarization, intracellular trypsin activation, and cell death. Notably, these effects were dependent on the degree and duration of force applied to the cell. Low or transient force were insufficient to activate these pathological changes whereas higher and prolonged application of force triggered sustained elevation in intracellular calcium leading to enzyme activation and cell death. All of these pathological events were rescued in acinar cells treated with a Piezo1 antagonist and in acinar cells from mice with genetic deletion of Piezo1. We discovered that Piezo1 stimulation triggered TRPV4 channel opening which was responsible for the sustained elevation in intracellular calcium that caused intracellular organelle dysfunction. Moreover, TRPV4 gene knockout mice were protected from Piezo1 agonist- and pressure-induced pancreatitis. These studies unveil a calcium signaling pathway in which Piezo1-induced TRPV4 channel opening causes pancreatitis.

Introduction

The pancreas is highly sensitive to pressure (1-3) and elevated pancreatic duct pressure is a major cause of acute pancreatitis. A gallstone impacted at the junction of the pancreatic and common bile ducts increases pancreatic duct pressure and can initiate pancreatitis (4-6). Intraductal pancreatic pressure is also increased during the clinical procedure endoscopic retrograde cholangiopancreatography (ERCP) when radiocontrast dye is injected into the pancreatic duct to visualize the pancreas (7). Acute pancreatitis develops in up to 20% of high risk patients undergoing this procedure (8). Mechanical injury to the pancreas through abdominal trauma is also a common cause of pancreatitis (9). Recently, our group demonstrated that the pancreatic acinar cell senses pressure through the mechanically-activated ion channel Piezo1 and activation of Piezo1 on acinar cells by pressure or a Piezo1-specific agonist, induced acute pancreatitis (1). Moreover, mice with acinar cell-specific deletion of Piezo1 were protected from pressure-induced pancreatitis. Thus, mechanical activation of Piezo1 is sufficient to cause pancreatitis.

Mechanical forces including static pressure, fluid shear stress, and membrane stretch activate Piezo1 channel opening which allow cations, most notably Ca^{2+}, to flow into the cell (10-14). Recently, Yoda1, a pharmacological agonist selective for Piezo1 but not Piezo2, has been identified (15). Piezo1 is expressed in numerous tissues that respond to shear force including the vascular endothelium, lung, skin, and urinary bladder (16, 17). Studying the signaling of Piezo1 in the pancreas offers an attractive model for unveiling the pathological response because of the uniquely sensitive behavior of pancreatic acinar cells to alterations in intracellular calcium levels.

Intracellular Ca^{2+} concentrations are tightly regulated in pancreatic acinar cells and provide the major signal for digestive enzyme secretion (18, 19). Cholecystokinin (CCK), acetylcholine and bombesin are pancreatic secretagogues that raise cytosolic calcium ($[Ca^{2+}]_i$) and thus stimulate secretion (20-22). Binding of these agonists to their

respective G-protein coupled receptors triggers the release of Ca^{2+} from the endoplasmic reticulum (ER) through increased activity of phosphoinositide-specific phospholipase C that cleaves phosphatidylinositol, 4,5-bisphosphate (PIP_2) to inositol 1,4,5-trisphosphate (IP_3) and diacylglycerol (23). Notably, this Ca^{2+} rise is necessary for normal cell signaling. Perturbation of Ca^{2+} signaling is associated with pancreatic acinar cell death (23). Supramaximal concentrations of agonists such as CCK lead to activation of calcium release activated channels (CRAC) in the plasma membrane (24) resulting in a sustained elevation in $[Ca^{2+}]_i$ and intracellular activation of proenzymes in pancreatic acinar cells that ultimately leads to cell death (24). Due to their intensive protein synthesis, acinar cells have high energy requirements and mitochondrial demands. Mitochondrial dysfunction can lead to impairment in energy requiring processes including proenzyme sorting, intracellular lysosome and zymogen vesicle formation and stability, and cellular integrity (25). Disruption of any of these functions can lead to pancreatitis. Calcium overload causes opening of the mitochondrial permeability transition pore (MPTP), collapses the mitochondrial membrane potential and disrupts the proton gradient necessary for ATP production which is required to satisfy the high energy demands of the acinar cell (25-29). Therefore, maintenance of proper mitochondrial function is necessary to prevent pancreatitis.

The calcium permeable ion channel, transient receptor potential vanilloid subfamily 4 (TRPV4), is expressed in various tissues and cells (e.g., smooth muscle of the urinary bladder, epithelial cells of kidney, airways, sensory neurons, and vascular endothelium) and is involved in several physiological processes and diseases including regulation of blood flow, shear-induced vasodilation and epithelial ciliary activity (30-37). TRPV4-mediated pathological events include neurogenic inflammation, hyperalgesia, endothelial dysfunction, and pulmonary and cardiac tissue fibrosis (33, 36, 38-40).

TRPV4 may be activated by physical force (e.g., shear stress, membrane stretching) and hypotonic cell swelling but this sensing appears to be indirect (41, 42). However, the mechanism by which these physical forces activate TRPV4 is not clear.

Hypotonic cell swelling and shear stress stimulate phospholipase A2 (PLA2) activity (42). In general, elevated phospholipase A2 activity triggers the release of arachidonic acid (AA) and its metabolite, 5′, 6′-epoxyeicosatrienoic acid (5′,6′-EET) (43). 5′, 6′-EET is an endogenous ligand that can activate TRPV4 (43). However, the mechanism by which physical stimuli activate PLA2 is not known. Phosphorylation of protein kinase A (PKA) and protein kinase C (PKC) increase the sensitization of TRPV4 (44, 45) therefore, it is possible that activation of TRPV4 through arachidonic acid may require PKA or PKC phosphorylation (44).

Here, we demonstrate that activation of Piezo1 in pancreatic acinar cells by direct chemical stimulation and fluid shear stress produced a sustained increase in cytosolic Ca^{2+}, followed by mitochondrial depolarization, and premature trypsinogen activation. Moreover, Piezo1-induced Ca^{2+} signaling is distinctly different from CCK-induced Ca^{2+} signaling suggesting that multiple pathways may contribute to the initiation of pancreatitis. To explain how Piezo1 activation led to sustained and pathological elevation in $[Ca^{2+}]_i$, we explored other potential calcium entry pathways and discovered that both mouse and human pancreatic acinar cells express the calcium permeable channel TRPV4. We also demonstrate that Piezo1 induced the activation of PLA2 which causes TRPV4 channel opening.

Results

Piezo1 induces sustained cytoplasmic Ca^{2+} elevation and cell death

In order to determine whether calcium signaling is responsible for the effects of Piezo1 on the pancreas, we first examined the ability of the chemical Piezo1 agonist Yoda1 to regulate intracellular calcium ($[Ca^{2+}]_i$) in freshly isolated pancreatic acini.

Changes in $[Ca^{2+}]_i$ were determined in acinar cells loaded with the calcium indicator Calcium 6-QF. We recently reported that the Piezo1 antagonist GsMTx4 inhibits the Yoda1-mediated $[Ca^{2+}]_i$ rise in pancreatic acini (1, 46). Here, we demonstrate the contribution of external and intracellular free calcium on Piezo1-mediated $[Ca^{2+}]_i$. Yoda1 in the presence of bath calcium (2 mM) produced an initial transient Ca^{2+} rise followed by sustained intracellular calcium elevation (Figure 1A and B and Movie 1). Removal of external calcium completely abolished the Yoda1-mediated $[Ca^{2+}]_i$ rise (Figure 1A and B). However, pre-incubating cells with BAPTA-AM (a cell-permeable Ca^{2+} chelator) for 30 minutes abolished the sustained Ca^{2+} rise (Figure 1C and D). Cholecystokinin (CCK) is a secretagogue that stimulates pancreatic enzyme secretion by increasing $[Ca^{2+}]_i$. In contrast to the effects on Yoda1-induced $[Ca^{2+}]_i$, preincubation of cells with BAPTA-AM completely eliminated the effect of CCK on $[Ca^{2+}]_i$ (Supplemental Figure S1).

To examine the effect of sustained Piezo1 activation on $[Ca^{2+}]_i$ and its relation to cellular injury, we treated pancreatic acini with Yoda1 and cellular injury was assessed by measuring lactate dehydrogenase (LDH) release. Cells were pre-incubated with or without BAPTA-AM. Chelating intracellular free calcium with BAPTA-AM protected pancreatic acini from Yoda1-induced LDH release (Figure 1F). We confirmed the specificity of these effects for Piezo1 by comparing the cytotoxic effects of CCK (Figure 1E). At high concentrations, CCK is well known to cause cell damage *in vitro* and pancreatitis *in vivo* (47, 48). As shown in Figure 1E, CCK produced comparable cell damage in pancreatic acini from both wild type mice and mice with selective genetic deletion of Piezo1 in pancreatic acinar cells ($Piezo^{aci}$ KO) mice (1). We visualized the effect of Yoda1 on pancreatic acini over time by live cell imaging. Application of Yoda1 (50 μM) caused swelling of wild type pancreatic acinar cells, release of zymogen granules from the basolateral surface and gradually ruptured the cell membrane (Figure

1G, Movie 2). Pancreatic acinar cells from Piezo1^{aci} KO mice did not respond to Yoda1 (Movie 3).

In pancreatic acinar cells, CCK at supraphysiological concentrations produces a sustained elevation of $[Ca^{2+}]_i$, the initial phase of which is due to release of Ca^{2+} from the endoplasmic reticulum (ER) (23). Following this initial rise, the sustained phase occurs through the activation of calcium release-activated channels (CRAC) which allows extracellular Ca^{2+} to flow into cells. In order to determine if the Piezo1-mediated sustained $[Ca^{2+}]_i$ elevation is due to CRAC activation, we examined the effects of the CRAC inhibitor, CM4620, which selectively inhibits Orai, the main component of CRAC (49). Pre-incubating acinar cells with CM4620 for 1 hour blocked the sustained elevation in $[Ca^{2+}]_i$ produced by CCK (100 and 1,000 pM) (Supplemental Figure S2A-C). Notably, CM4620 did not completely block the $[Ca^{2+}]_i$ rise induced by either concentration of CCK and a residual calcium wave was always observed following CCK despite CM4620 administration (Supplemental Figure S2A-C). This persistent calcium wave was possibly due to Ca^{2+} released from endoplasmic reticulum (ER) stores (50, 51). In contrast to the effects on CCK-stimulated $[Ca^{2+}]_i$, CM4620 did not alter the rise in $[Ca^{2+}]_i$ following Yoda1 stimulation (Supplemental Figure S2D and E) indicating that CRAC channels are not the source of sustained $[Ca^{2+}]_i$ elevation following Piezo1 activation.

To determine if Piezo1 gene deletion altered the acinar cell response to secretagogue stimulation, we examined the effects of CCK on $[Ca^{2+}]_i$ in pancreatic acini from Piezo1^{aci} KO mice. Pancreatic acini from wild type and Piezo1^{aci} KO mice responded equally to both physiological (20 pM) and supraphysiological (1 nM) CCK concentrations (Supplemental Figure S3A-D). In order to confirm that Piezo1 and CCK stimulate $[Ca^{2+}]_i$ through distinct mechanisms, we first activated Piezo1 channels in pancreatic acini through mechanical force by applying a blunt glass pipette to the surface of acinar cells to a depth of 5 μm for 1 second. This blunt pushing produced a

transient $[Ca^{2+}]_i$ elevation. Cells were then exposed to CCK (20 pM). Slight mechanical pushing did not alter the sensitivity of pancreatic acini to subsequent CCK exposure (Supplemental Figure S3E and F). In light of the finding that Piezo1 and CCK affect $[Ca^{2+}]_i$ through separate pathways, we sought to determine if together Yoda1 and CCK accentuated the deleterious effects on pancreatic acinar cells. Compared to individual application of Yoda1 and CCK, acinar cell death was greater when cells were exposed to both Yoda1 and CCK (Supplemental Figure S3G and H).

Piezo1 agonist, Yoda1, induces pathological events in pancreatic acini

Pancreatic acinar cells possess abundant mitochondria and are highly metabolically active. Proper mitochondrial function is critical for cellular homeostasis and mitochondrial dysfunction has been implicated in the pathogenesis of pancreatitis. We postulated that the elevations in cytoplasmic $[Ca^{2+}]$ that were observed with Yoda1 stimulation and Piezo1 activation in pancreatic acinar cells may affect mitochondrial depolarization. To test this hypothesis, we used a cell-permeable and mitochondrial potential-sensitive fluorescent dye, tetramethyl rhodamine ester (TMRE) (52, 53). TMRE accumulates as punctate distributions in mitochondria due to high negative membrane potential. The fluorescence intensity of this punctate pattern declines following mitochondrial depolarization. Application of Yoda1 (50 μM) throughout the period of live cell imaging significantly decreased TMRE fluorescence intensity indicative of depolarization of the mitochondria (Figure 2A-C). GsMTx4 blocked the Yoda1-induced mitochondrial depolarization in wild type cells. Yoda1 did not depolarize mitochondria in $Piezo1^{aci}$ KO cells (Figure 2B and C). Pancreatic acinar cells pre-incubated with BAPTA-AM for 20 minutes were protected from Yoda1-induced mitochondrial depolarization, suggesting a significant role for intracellular free calcium (Figure 2E). We observed that Yoda1-induced mitochondrial depolarization occurred at a higher rate than that induced with CCK (10 nM) (Figure 2A-D). Yoda1-mediated

mitochondrial depolarization occurred within 3 minutes of application, however, CCK mediated mitochondrial depolarization occurred more slowly and was observed only after 10 minutes of drug exposure.

Premature zymogen activation and auto-digestion of acinar cells are critical events in pancreatitis. Moreover, pathophysiological elevations in cytoplasmic [Ca^{2+}] have been associated with intracellular trypsinogen activation (52, 54). We postulated that prolonged activation of Piezo1 may cause trypsinogen activation through a calcium-mediated pathway. We visualized real-time trypsinogen activation in pancreatic acini using a trypsin-sensitive, cell-permeable fluorescent probe, BZiPAR, that becomes fluorescent once it is cleaved specifically by trypsin (52, 55). Application of either Yoda1 (50 μM) or CCK (10 nM) activated trypsin in pancreatic acini over time (Figure 2F and G and Movie 4). Yoda1 induced trypsin activation within 10 minutes of application, however CCK stimulated trypsin activation more slowly and was observed only after 20 minutes of drug exposure (Movie 4). GSMTx4 blocked the Yoda1-induced trypsin activation in pancreatic acinar cells (Figure 2H). Pancreatic acinar cells from Piezo1^{aci} KO mice did not respond to Yoda1 (Figure 2H). Furthermore, CCK mediated trypsin activation was similar in acini from wild type and Piezo1^{aci} KO mice (Figure 2I).

Mechanical pushing- and shear stress-induced $[Ca^{2+}]_i$ elevation in pancreatic acini

Mechanical activation of Piezo1 in acinar cells was demonstrated by applying a blunt glass pipette to the surface of acinar cells to a depth of 5 μm for 1 second. This stimulation produced a transient $[Ca^{2+}]_i$ rise (Figure 3A and B and Movie 5) that was completely blocked by prior treatment of the cells with GsMTx4 (Figure 3C). In addition, mechanical pushing did not increase $[Ca^{2+}]_i$ in acinar cells from Piezo1^{aci} KO mice (Figure 3C and Movie 6). Removal of external calcium blocked the mechanical pushing-mediated $[Ca^{2+}]_i$ rise (Figure 3D). In order to apply physical force for a longer

time, we used a fluid shear stress approach to avoid cell damage that might occur with repeated mechanical pushing and other technical difficulties. The fluid shear stress approach is similar to the situation in which high fluid pressure is injected into the pancreatic duct as we have demonstrated (1) which has been used as a model for the clinical condition of excess filling of the pancreatic duct in humans during endoscopic retrograde cholangiopancreatography (ERCP) (7).

Mechanical shear stress is a physiological activator of Piezo1 in many tissues including vascular endothelium (12, 13). To determine if Piezo1 channels are responding to fluid shear stress in the pancreas, we evaluated changes in $[Ca^{2+}]_i$ in freshly isolated pancreatic acini plated in a shear flow chamber (13). Following a period as brief as 30 seconds, the peak intensity of $[Ca^{2+}]_i$ in pancreatic acini increased as greater shear stress forces were applied (Figure 3E and F). Shear stresses of 4, 12, and 30 dyne/cm^2 increased the peak $[Ca^{2+}]_i$ by 1.5±0.1, 1.8±0.1 and 2.5±0.1 fold, respectively (Figure 3E and F). The 12 and 30 dyne/cm^2 stresses caused a sustained elevation in $[Ca^{2+}]_i$ and mimicked the $[Ca^{2+}]_i$ pattern induced by Yoda1 (25 μM and 50 μM) (Figure 3E, Figure 1A and C). However, the lower shear stress force of 4 dyne/cm^2 elicited only a transient $[Ca^{2+}]_i$ rise (Figure 3E) without a prolonged $[Ca^{2+}]_i$ elevation. Furthermore, fluid shear stress force of 12 dyne/cm^2 applied for 1 second or 5 seconds was not sufficient to induce a sustained elevation in $[Ca^{2+}]_i$ (Figure 3G and H). The sustained $[Ca^{2+}]_i$ elevation at 12 dyne/cm^2 did not occur in pancreatic acini from Piezo1^{aci} KO mice although small transient $[Ca^{2+}]_i$ peaks at regular intervals could be seen in some cells (Figure 3I and J). We suspect that small transient spikes in $[Ca^{2+}]_i$ occurring at regular intervals could be from low expression of other mechanically-sensitive channels.

Fluid shear stress induces pathological events in pancreatic acini

To determine whether fluid shear stress-activated Piezo1 facilitates mitochondrial depolarization, we monitored live cell mitochondrial depolarization in

pancreatic acini loaded with the mitochondrial sequestrant dye, TMRE (200 nM), from wild type and Piezo1^{aci} KO mice. Fluid shear stress administered at 12 dyne/cm^2 for 30 seconds that caused a sustained elevation in $[Ca^{2+}]_i$ decreased the TMRE intensity over time in wild type pancreatic acini but not in Piezo1^{aci} KO cells (Figure 4A and B). In these experiments fluid shear stress led to a sustained depolarization consistent with a state of mitochondrial dysfunction (Movie 7) (25, 56). The mitochondrial potential of pancreatic acini with Piezo1 deletion was not affected by these conditions of fluid shear stress (Figure 4B, Movie 7). These results demonstrate that Piezo1 channels mediate fluid shear stress-induced mitochondrial depolarization. In contrast, mechanical pushing of acinar cells with a glass pipette only slightly depolarized the mitochondria in 20% of acinar cells while the remainder were completely unaffected. Overall, it appears that pushing of pancreatic acinar cells once for 1 second was not sufficient to substantially depolarize the mitochondria (Supplemental Figure S4A).

Pancreatic enzyme activation in pancreatic acinar cells is a key pathological feature in pancreatitis. As reported here, the Piezo1 agonist Yoda1 induces trypsinogen activation which is the initial step in activation of other zymogens in the pancreas. To determine if fluid shear stress mimics the Yoda1 effect and trypsin activation, pancreatic acinar cells were loaded with the trypsin activity measuring probe BZiPAR. Pancreatic acini were then subjected to fluid shear stress at 12 dyne/cm^2 for 30 seconds. Trypsin activity monitored by live cell imaging was detected after 10 minutes of fluid shear stress and gradually increased for up to 50 minutes (Figure 4C). An increase in BZiPAR dye (trypsin activity) was not observed in Piezo1^{aci} KO cells. In contrast, however, a short pulse of 5 seconds, instead of 30 seconds, at a force of 12 dyne/cm^2 did not trigger trypsin activation in wild type acinar cells (Figure 4D). As we observed with mitochondrial depolarization, brief mechanical pushing of pancreatic acinar cells was not sufficient to activate trypsin (Supplemental Figure S4B).

Piezo1 mediates TRPV4 channel activation in pancreatic acini

Although Piezo1 is a fast inactivating channel, fluid shear stress and Yoda1 caused a sustained elevation in $[Ca^{2+}]_i$ raising the possibility that other calcium entry channels or Piezo1-mediated downstream signaling pathways may exist. CRAC which is expressed in pancreatic acinar cells (24) was one possibility, however, we observed that the CRAC inhibitor CM4620, which selectively inhibits the Orai channel, blocked the sustained elevation in $[Ca^{2+}]_i$ produced by CCK but not that induced by Yoda1 (Figure S2). Therefore, it is unlikely that CRAC contributes to Piezo1-stimulated Ca^{2+} entry. Since TRPV4 indirectly senses fluid shear stress, we sought to determine if TRPV4 was expressed in pancreatic acinar cells. As shown in Figure 5A and B, TRPV4 mRNA and protein were detected by RT qPCR and immunostaining, respectively. Moreover, TRPV4 is highly expressed in both mouse and human pancreatic acini (Figure 5A and B, Supplemental Figures S5A and S5C). Like mouse pancreatic acini, Piezo1 is also expressed in human pancreatic acini (Supplemental Figure S5B). In order to evaluate the function of TRPV4 in pancreatic acini, we used the TRPV4 channel agonist GSK10167790A (GSK101) and TRPV4 receptor antagonists HC067047 (HC067) and RN1734 (31, 32, 57). GSK101 (50 nM) induced a significant increase in $[Ca^{2+}]_i$ which was inhibited by both HC067 (100 nM) and RN1734 (30 μM) (Figure 5C and D).

To determine the mechanism for TRPV4 activation, we examined the PLA2 pathway by first testing the endogenous arachidonic acid (AA) metabolite ligand 5, 6-epoxyeicosatrienoic acid (5′, 6′-EET). Similar to the TRPV4 agonist GSK101, AA and 5′-6′ EET induced significant increases in $[Ca^{2+}]_i$ (Figure 5E and F) which were inhibited by the TRPV4 antagonist HC067 (Figure 5E and F). We next sought to determine if the ability of shear stress to produce the sustained elevation in $[Ca^{2+}]_i$ was due to TRPV4 by measuring $[Ca^{2+}]_i$ following shear stress (12 dyne/ cm^2 for 30 sec) in the presence of the TRPV4 antagonist, HC067. HC067 (1 μM, the concentration used to completely inhibit TRPV4 activity) (31) blocked the sustained $[Ca^{2+}]_i$ elevation leaving only transient

alterations in $[Ca^{2+}]_i$ (Figure 5G and H). Like shear stress experiments, HC067 completely blocked the Yoda1 (25 μM) stimulated sustained increase in $[Ca^{2+}]_i$ (Figure 5I and J). Importantly, we discovered that neither Yoda1 nor fluid shear stress (12 dyne/ cm^2 for 30 sec) caused a sustained increase $[Ca^{2+}]_i$ in pancreatic acini isolated from TRPV4 KO mice (Figure 5K and L). Together these findings indicate that Piezo1 directly senses fluid shear stress and initiates calcium influx. However, the activation of TRPV4 is responsible for the secondary sustained influx of calcium resulting in the sustained elevation in $[Ca^{2+}]_i$.

Piezo1 elevates phospholipase A2 activity

TRPV4 is activated by 5'- 6' EET generated through the PLA2-arachidonic acid cytochrome P450 epoxygenase dependent pathway (42). If this pathway is responsible for Piezo1-initated TRPV4 channel activation then Yoda1 should be able to induce PLA2 activation. To test this hypothesis, acinar cells were loaded with the fluorogenic PLA2 substrate (Bis-BODIPY™ FL C_{11}-PC) (1, 2-Bis (4, 4-Difluoro-5, 7-Dimethyl-4-Bora-3a, 4a-Diaza-*s*-Indacene-3-Undecanoyl)-*Sn*-Glycero-3-Phosphocholine). Prior to Yoda1 stimulation, initial Bis-BODIPY™ FL C_{11}-PC loaded pancreatic acini exhibited only faint fluorescence. However, application of Yoda1 markedly increased the intensity of the fluorogenic phospholipase A2 (PLA2) substrate indicating that Piezo1 is able to induce the PLA2 activity (Figure 6A and B, Movie 8). The effects of Yoda1 were observed within 30 seconds of application and reached a plateau after 4 minutes (Figure B). Yoda1 did not stimulate PLA2 activation in pancreatic acini from $Piezo1^{aci}$ KO mice (Figure 6B and C). To confirm that the increase in PLA2 activity was responsible for the Piezo1-induced sustained $[Ca^{2+}]_i$ levels, we tested the secretory and cytosolic phospholipase A2 inhibitors YM26734 and AACOCF3, respectively (58, 59). Together YM26734 and AACOCF3 blocked the Yoda1-induced sustained $[Ca^{2+}]_i$ elevation indicating that Piezo1 induced PLA2 which was responsible for the subsequent $[Ca^{2+}]_i$

elevation (Figure 6D and E). However, only the secretory PLA2 inhibitor effect was substantial and capable of blocking the sustained $[Ca^{2+}]_i$ elevation (Figure 6D and E). Protein kinase A and C inhibitors did not significantly affect Yoda-stimulated $[Ca^{2+}]_i$ (Supplemental Figure S6).

TRPV4 KO mice are protected against pressure-induced pancreatitis

Sustained elevations in $[Ca^{2+}]_i$ are sufficient to cause pancreatitis (60). Having demonstrated that Piezo1-initiated, sustained $[Ca^{2+}]_i$ elevation requires TRPV4 activation, we proposed that TRPV4 KO mice could be protected from Piezo1-mediated pancreatitis. In order to selectively stimulate Piezo1 in the pancreas, Yoda1 (0.4 mg/kg) was infused into the pancreatic duct at a rate of 5 μL/min (Figure 7A). This rate of infusion did not exceed the pancreatic duct pressure of 11 mm Hg and is considered a low pressure condition (1) that alone does not cause pancreatitis. As shown in Figure 7B-F, Yoda1 infusion increased all pancreatitis parameters measured (pancreatic edema, serum amylase, pancreatic myeloperoxidase (MPO), and histological scoring) in wild type mice. In contrast, the same dose of Yoda1 did not cause pancreatitis in TRPV4 KO mice (Figure 7B-F).

Having demonstrated that Piezo1 and CCK increase $[Ca^{2+}]_i$ through separate mechanisms, we proposed that CCK would not trigger TRPV4 channel opening. In support of this idea, we found that the TRPV4 channel blocker HC067 did not affect the CCK (1 nM) stimulated peak or sustained $[Ca^{2+}]_i$ changes (Supplemental Figure S7A-C). It follows then that if CCK does not stimulate TRPV4 opening in acini, TRPV4 KO mice would not be protected from caerulein-induced pancreatitis. As expected, caerulein-induced pancreatitis was similar in both wild type and TRPV4 KO mice (Supplemental Figure S7D-H).

Piezo1 is responsible for pressure-induced pancreatitis (1). Experimentally, $Piezo1^{aci}$ KO mice were protected against pancreatitis caused by high intrapancreatic

duct pressure (1). If the pathological effects of Piezo1 activation are due to the downstream activation of TRPV4, we would expect that mice lacking TRPV4 would be protected against pressure-induced pancreatitis. We induced pancreatitis by ligating the tail region of the pancreas up to 24 hours (Figure 7G). In wild type mice, pancreatic duct ligation caused acute tissue injury which was reflected by an increase in all pancreatitis parameters. In contrast, TRPV4 KO mice were protected against duct ligation-induced pancreatitis (Figure 7H-L). These findings confirm that TRPV4 plays a key role in pressure-induced pancreatitis.

Discussion

Acinar cells comprise 90% of the pancreas and are notable for their abundant digestive enzymes which render the gland highly susceptible to pancreatitis should enzymes become prematurely activated following organ damage. Intracellular enzyme activation is a hallmark of pancreatitis and is believed to play a central role in disease pathogenesis. Recently we demonstrated that pressure activation of Piezo1 channels in pancreatic acinar cells is responsible for pressure-induced pancreatitis (1). Prior to the identification of Piezo1 in acinar cells, it was not known how the pancreas senses pressure although a number of pathological situations indicate that the gland is exquisitely sensitive to pressure-induced injury. For example, intrapancreatic duct pressure is increased by occlusion of the pancreatic duct (4-6) and this is thought to be a key factor in the development of gallstone-induced pancreatitis which is one of the major causes of acute pancreatitis in humans. In this disease, impaction of a gallstone in the ampulla of Vater causes an abrupt increase in pancreatic duct pressure leading to pancreatitis (61). In addition, mechanical force on the pancreas during trauma or pancreatic surgery may cause pancreatitis (7, 9). Finally, injection of fluid into the pancreatic duct at high pressure during ERCP is a well-known cause of pancreatitis (7, 62, 63). In each of these causes of pancreatitis, abnormal pressure on the pancreas has

the potential to activate Piezo1. However, Piezo1 is also expressed in other tissues where it mediates several physiological processes like micturition, endothelial shear stress, embryogenesis, and vascular development (12, 13, 16, 17, 64). The question, therefore, arises how activation of the Piezo1 channel leads to the pathological process of pancreatitis? In general, under normal physiological conditions activation of Piezo1 channels is tightly regulated. Piezo1 channel function and transduction properties vary with stimulus frequency, waveform, and duration (65). We propose that overactivation of Piezo1 by persistent pressure or mechanical force in acinar cells produces downstream signaling events that disrupt normal cellular homeostasis resulting in premature enzyme activation and ultimately pancreatitis. In the pancreas, disruption of calcium homeostasis is detrimental and leads to pancreatitis (23, 66).

Here, we demonstrated that either chemical (Yoda1) or physical (shear stress) activation of Piezo1 induced $[Ca^{2+}]_i$ overload, caused mitochondrial dysfunction and led to intrapancreatic trypsinogen activation. Persistent application of the Piezo1 agonist Yoda1 at doses of 25 μM and 50 μM produced a sustained increase in $[Ca^{2+}]_i$ in pancreatic acini. A similar increase in $[Ca^{2+}]_i$ was seen when cells were subjected to fluid shear stress > 12 dyne/cm^2 for 30 seconds. However, mechanical pushing of the acinar cell surface up to 5 μm for 1 second caused only a transient rise in $[Ca^{2+}]_i$ and did not induce trypsinogen activation. Similarly, fluid shear stress at low pressure (4 dyne/cm^2) or for a short duration (1 or 5 seconds) did not induce these changes. It has been established previously that a sustained elevation in $[Ca^{2+}]_i$ in acinar cells is a prime cause of pancreatic injury (23, 66). Elevated $[Ca^{2+}]_i$ in pancreatic acinar cells produced by persistent Yoda1 exposure resembles that produced by supraphysiological doses of CCK, a well-known agent for inducing experimental pancreatitis (66). Thus, it seems reasonable to attribute the ability of Yoda1 to induce pancreatitis to its prolonged effects on $[Ca^{2+}]_i$. It is possible that brief push stimulation activates a subset of Piezo1 and

chemical activation acts on all channels which mimics the prolonged high shear stress mediated pathological effects.

We observed that removal of external Ca^{2+} abolished the Piezo1-mediated increase in $[Ca^{2+}]_i$ and pre-incubating cells with the cell permeable calcium chelator (BAPTA-AM) blocked the sustained increase in $[Ca^{2+}]_i$. Thus, it is possible that not only is external Ca^{2+} necessary for the Piezo1-mediated increase in $[Ca^{2+}]_i$ but this increase is required for the opening of a Ca^{2+} entry pathway that contributes to the sustained elevation in $[Ca^{2+}]_i$. This is consistent with the observation that pre-incubating cells with BAPTA-AM protected acini from Piezo1-mediated cellular injury. Notably, Piezo1-mediated stimulation of $[Ca^{2+}]_i$ differs from the CCK-mediated pathway. The Piezo1 pathway requires external Ca^{2+} to initiate the process whereas CCK stimulation begins via the release of Ca^{2+} from intracellular endoplasmic reticulum stores (23, 67).

Under physiological conditions, the pancreatic secretagogues acetylcholine and CCK stimulate $[Ca^{2+}]_i$ in a spatiotemporal manner that is required for ATP production, initiation of exocytosis, and nuclear signaling processes (68). However, supraphysiological CCK stimulation, excess ethanol, bile, and toxins induce a sustained elevation in $[Ca^{2+}]_i$ in pancreatic acinar cells that cause acute pancreatitis (28, 69-72). This sustained elevation in $[Ca^{2+}]_i$ mediates mitochondrial dysfunction, premature zymogen activation, vacuolization and necrosis (73). We observed that both Yoda1 and fluid shear stress induced mitochondrial depolarization and trypsin activation in pancreatic acinar cells. Transient depolarization of mitochondria following a rise in $[Ca^{2+}]_i$ is associated with normal cellular ATP production. However $[Ca^{2+}]_i$ overload in acinar cells induced by bile and ethanol (27, 28, 71, 74) opens the mitochondrial permeability transition pore (MPTP), collapses the mitochondrial membrane potential (ψm) required for ATP synthesis (75-77), and ultimately results in cell death. By chelating intracellular free Ca^{2+}, we prevented Yoda1-induced mitochondrial depolarization and cell death. It has been observed previously that intracellular

calcium chelation prevents zymogen activation (52, 78) and protects against acute pancreatitis *in vivo* (79). We observed that Piezo1-mediated mitochondrial depolarization preceded trypsin activation following either Yoda1 treatment or shear stress and is ultimately responsible for pressure-induced pancreatitis.

Piezo1 is a fast inactivating channel with single-channel conductance of ~22 pS (inward current) which is lower than the TRPV4 ion channel of ~60 pS (10, 80). Piezo1 inactivation kinetics are independent of stimulus intensity (10). If no other type of channels are present in the cell except Piezo1, the calcium rise will be transient rather than sustained due to fast inactivation kinetics. This suggests that the Piezo1-induced sustained elevation in $[Ca^{2+}]_i$ produced by Yoda1 or shear stress requires an extra calcium entry pathway. We, therefore, sought other potential channels that could be linked to Piezo1 activity and discovered that TRPV4 is expressed in both mouse and human pancreatic acini.

Initially, we thought that mechanical activation of Piezo1 and TRPV4 were independent processes. Even though activation of Piezo1 could produce a transient increase in $[Ca^{2+}]_i$, and TRPV4 could produce more sustained elevation of $[Ca^{2+}]_i$, by virtue of its slow inactivation kinetics and considerably higher single channel conductance, it was not clear if the two processes were linked. Remarkably, the TRPV4 antagonist HC067 completely blocked the sustained phase of calcium elevation induced by Yoda1 and shear stress. This provided the hint that Piezo1 regulates TRPV4 channel activation. The results were confirmed in experiments from TRPV4 KO mice when both Yoda1 and prolonged shear stress produced only transient elevation in $[Ca^{2+}]_i$. Low shear stress for 30 seconds and high shear stress for 5 seconds were not sufficient to induce a sustained calcium rise and did not activate TRPV4. The reason could be the brief force caused only a subset of Piezo1 channel openings and was insufficient to activate PLA2. In the cell, PLA2 is activated upon binding to calcium ions that accelerates enzyme activity, which initiates the arachidonic pathway and TRPV4

channel activation. In mouse pancreatic acinar cells, the Piezo1 agonist, Yoda1 increased PLA2 activity and caused a sustained elevation in $[Ca^{2+}]_i$, an effect that was inhibited by a PLA2 inhibitor. Various reports indicate that TRPV4 is sensitive to mechanical stimuli such as osmotic pressure, shear stress and mechanical stretching (31-37). However, it was unclear how mechanical stimuli actually activate the TRPV4 channel. The current findings indicate that Piezo1 stimulation of PLA2 and subsequent activation of TRPV4 could be a mechanism by which TRPV4 channels respond to mechanical force.

Supramaximal doses of CCK secretagogue block apical secretion and cause intracellular vacuolization, enzyme activation and enzyme release from the basolateral surface of the cell (81, 82). In the present study we observed that Yoda1 induced the release of vesicles from the basolateral surface indicating a possible pathological situation.

We did not observe any significant effects of PKA and PKC inhibitors on Yoda1-mediated TRPV4 activation. In other cells such as HEK293 cells or human coronary artery endothelial cells, PKA and PKC can directly phosphorylate TRPV4 and modify channel activity. Our findings suggest that this pathway is not required for channel activation.

The current study demonstrates that Piezo1 initiates the pressure-induced calcium signal causing TRPV4 activation but the pathological events that occur in the acinar cell require TRPV4-mediated calcium influx which is responsible for the sustained phase of calcium elevation that leads to pancreatitis. Consistent with this pathological sequence of events, TRPV4 KO mice were protected from Yoda1-induced pancreatitis.

To mimic pancreatitis caused by pancreatic duct obstruction (e.g., gallstones), we used a mouse model of pancreatitis by ligating the tail region of the pancreas for 24 hours (83). In this model, we observed that TRPV4 KO mice were significantly

protected. Hence, a TRPV4 channel blocker could be a possible treatment for pancreatitis where pressure is encountered.

Our findings suggest the activation of Piezo1 in the absence of TRPV4 is not sufficient to induce pathological calcium signaling. However, when co-expressed and linked by intracellular signaling pathways, TRPV4 may appear to be pressure-sensitive. For example, Piezo1 and TRPV4 channels are expressed in endothelial cells and previous reports have indicated that high pulmonary venous pressure induces Ca^{2+} influx into endothelial cells via TRPV4 channels resulting in increased vascular permeability which is a major cause of mortality in heart failure patients (33). Although unrecognized at the time, this process may be linked to Piezo1 which appeared to sense high vascular pressures at the lung endothelial surface and account for vascular hyperpermeability and pulmonary edema (30). Thus, it appears that both Piezo1 and TRPV4 are responsible for this vascular hyperpermeability and our findings suggest that they may be linked. We hypothesize that Piezo1 sensing of high vascular pressure initiates a Ca^{2+} signaling pathway that triggers the activation of TRPV4. TRPV4 activation would then cause a secondary, sustained Ca^{2+} influx that would lead to vascular hyperpermeability. The extent of TRPV4-induced Ca^{2+} entry would be influenced by other factors including the level of TRPV4 expression, the degree and duration of pressure, and, if identical to the pancreas, the appropriate level of PLA2 activity. Thus, our findings may represent a more generalized process in which TRPV4 converts Piezo1 pressure sensing into a pathological event.

Methods

Animals. Targeted deletion of Piezo1 in pancreatic acinar cells was accomplished as follows. *Piezo1*$^{fl/fl}$ mice were a gift from A. Patapoutian, Department of Neuroscience, Scripps Research, La Jolla, California (84) and were crossed with *ptf1*$^{atm2\ (cre/ESR1)\ Cvw\ /J}$ mice (Jackson Labs) to generate the mouse line *ptf1a*^{CreERTM}; *piezo1*$^{fl/fl}$. *Piezo1*$^{fl/fl}$ mice were used

as wild type and the *ptf1a*^{CreERTM}*; piezo1*$^{fl/fl}$ mice at the age of 5-7 weeks were subjected to 1 mg of tamoxifen (Sigma #T5648) injected intraperitoneally for five consecutive days. After tamoxifen induction the *ptf1a*^{CreERTM}*; piezo1*$^{fl/fl}$ mice expressed a truncated Piezo1 specific to pancreatic acinar cells and are referred to as Piezo1^{aci} KO mice. Eight days after the last tamoxifen injection, mice were used in experiments and each time a small piece of pancreas was used for genotyping. Mice (both male and female) aged 7 -12 weeks were used in the experiments. *Piezo1*$^{fl/fl}$ mice (8-12 weeks of age) on a C57BL/6J background (1) were used as wild type mice and *ptf1a*^{CreERTM}*; piezo1*$^{fl/fl}$ mice after tamoxifen injection were used as Piezo1^{aci} KO mice for experiments with the Piezo1 agonist, Yoda1, and shear stress. C57BL/6J mice (8–14 weeks old) were used as wild type mice and mice with *trpv4*$^{-/-}$ gene deletion (referred to as TRPV4 KO) received from Wolfgang Liedtke, Department of Neurology, Duke University, Durham, North Carolina (85) backcrossed on a C57BL/6J background, were used for both Yoda1 and partial duct ligation-mediated pancreatitis experiments. For *in vivo* experiments with Yoda1, wild type mice were also injected with tamoxifen. Mice were housed under standard 12:12 h light-dark periods and experimental protocols and studies were performed with approval from the Institutional Animal Care and Use Committee of Duke University.

Pancreatic acini and acinar cell preparations. Mouse pancreatic acini were isolated using the standard collagenase digestion protocol as previously described (1, 86, 87). Isolated acini were plated on a thin layered Matrigel coated glass bottom culture plate (MatTek**,** P35G-0-14-C). Freshly isolated acini were used in each experiment.

Shear stress assays. Parallel-plate fluid flow chambers (μ-Slide I 0.4 Luer, and μ-Slide I 0.2 Luer from Ibidi GmbH, Germany) were used to measure the shear stress-induced changes in intracellular calcium, mitochondrial depolarization, and trypsin activation

(13). The constant flow rate with shear stress (τ) is given by $\tau = \eta \times 104.7.6\ \varphi$ for μ-Slide I 0.4 Luer, and $\tau = \eta \times 330.4\ \varphi$ for μ-Slide I 0.2 Luer; η: viscosity of the medium; φ: flow rate (according to the manufacturer's instructions, Ibidi).

Mechanical Pushing. A borosilicate glass pipette (Sutter Instrument) was pulled using a pipette puller P-87 (Sutter Instrument) and made blunt with a MF-900 Microforge (Narishige, Japan). Acini were pushed once with a 2-3 μm tip blunt pipette to 5 μm for 1 second using a micromanipulator (World Precision Instruments).

Calcium Imaging. Calcium imaging in pancreatic acini were was performed as described previously (1). The chemicals used in calcium imaging experiments included: Yoda1 (Tocris; 5586), GsMTx4 (Abcam; ab141871), 5,6- eicosatrienoic acid (Santa Cruz Biotechnology; sc-221066), arachidonic acid (Sigma; A3611), HC067047 (Tocris; 4100), GSK1016790A (Sigma; G0798), RN1734 (Tocris; 3746), AACOCF3 (Tocris; 1462), YM26734 (Tocris; 2522), and GF109203X (Tocris; 0741) and CCK8 from Sigma-Aldrich.

Mitochondrial depolarization. Live cell mitochondrial depolarization was analyzed according to the previously described protocol (52) using the mitochondrial labeling dye TMRE (tetramethylrhodamine, ethyl ester). Isolated acini were plated on a thin layered Matrigel coated glass bottom culture plate with DMEM/F12 and 10% FBS media and placed in a CO_2 incubator for 1 hour at 37°C. After 1 hour the acini were incubated with TMRE (200 nM) in the bath buffer containing (in mM): 140 NaCl, 4.7 KCl, 2.0 $CaCl_2$, 1 $MgCl_2$, 10 HEPES, 10 glucose (pH adjusted to 7.4 with NaOH) for 30 minutes. The TMRE dye was washed and replaced with fresh bath buffer. The images were captured with a Zeiss Axio observer Z1 microscope with MetaMorph software (Molecular Devices) at intervals of 600 ms. TMRE was excited at 540-600 nm and emission collected at 585-675 nm. FCCP (carbonyl cyanide 4-(trifluoromethoxy)

phenylhydrazone) that uncouples the oxidative phosphorylation process and depolarizes mitochondria was used as a positive control (52, 53). A maximum of two mitochondrial puncta was taken per acinar cell (53).

Trypsinogen activation. To visualize the Piezo1-induced trypsinogen activation, acini were loaded with active trypsin enzyme substrate BZiPAR [rhodamine 110, bis(CBZ-L-isoleucyl-L-prolyl-L-arginine amide)] (10 μM) (52, 55). Na-Hepes buffer with 2 mM Ca^{2+} was used during imaging. A Zeiss Axio observer Z1 with a high sensitivity-EMCCD camera with a 40x/0.75 EC-Plan-NeoFluar DIC objective was used to capture the Z-stack images with stack thickness of 3 μm at an interval of 12 seconds. The BZiPAR fluorescent wavelength, Ex/Em was 498/521 nm. BZiPAR was excited at 470-510 nm and emission collected at 495-550 nm. The captured images were analyzed with MetaMorph software (Molecular Devices).

Cell death assays. The viability of pancreatic acini with Yoda1 and CCK treatments was analyzed using the Live/Dead cell imaging kit from ThermoFisher Scientific, Catalog # R37601 (88) or lactate dehydrogenase release assay kit from Promega, Catalog # G1780 (1).

Phospholipase A2 activity. The fluorogenic phospholipase A2 (PLA) substrate (Bis-BODIPY™ FL C_{11}-PC) (1,2-Bis (4,4-Difluoro-5,7-Dimethyl-4-Bora-3a, 4a-Diaza-*s*-Indacene-3-Undecanoyl)-*Sn*-Glycero-3-Phosphocholine) from ThermoFisher Scientific; B7701) was used to monitor the phospholipase A2 activity in living cells. The pancreatic acini were incubated with Bis-BODIPY™ FL C_{11}-PC in HBSS buffer with 2 mM Ca^{2+} for 30 minutes. HBSS buffer with 2 mM Ca^{2+} was used during imaging. A Zeiss Axio observer Z1 with a high sensitivity-EMCCD camera with a 40x/0.75 EC-Plan-NeoFluar DIC objective was used to capture the Z-stack images

with stack thickness of 4 μm at an interval of 10 seconds with a 480 nm excitation and 525-nm emission filter. The captured images were analyzed with MetaMorph software (Molecular Devices).

Immunostaining. Pancreatic acini were incubated with a rabbit anti-TRPV4 antiserum (Alomone; #ACC-034; 1:250) or with a rabbit anti-Piezo1 antiserum (Alomone; # APC-087; 1:300) overnight at 2-8°C. The signals from TRPV4 and Piezo1 immunostaining were amplified by the tyramide signal amplification method using a kit (Life Technologies; #T20924) following the manufacturer's instructions. The nuclei were stained with Nunc blue (Invitrogen; R376060). All staining images were taken with a Zeiss Axio observer Z1 with a 20x objective or a ×63 oil-immersion objective.

***In vivo* pancreatitis models.** Laparotomy surgery was performed both in pancreatic partial duct ligation and retrograde pancreatic duct infusion-mediated pancreatitis experiments as previously described (1). Yoda1 at dose of 0.4 mg/kg in 50 μL was injected as previously described (1). In Yoda1-mediated pancreatitis, the mid-portion of the pancreas (about 100-125 mg) was carefully excised and used for biochemical assays and histological staining. Histological scoring was evaluated from the entire section. Partial pancreatic duct ligation (PDL) was done as previously described (89, 90). Using a stereo microscope the tail region of the pancreas was visualized and the main pancreatic duct was ligated carefully with 6-0 Prolene suture without damaging the left portal vein that separates the splenic lobe and gastroduodenal part of the pancreas. Any mice suffering damage to any underlying blood vessels were excluded from the experiment. The pancreas was examined 24 hrs after ligation. A 100-125 gm portion of the tail region of the pancreas was used for biochemical assays and histological staining. Mice were subjected to caerulein-induced pancreatitis by intraperitoneal injection of

caerulein (50 μg/kg) (Tocris; catalog #6264) every hour for a total of 6 injections as previously described (85).

Blood amylase assay. The serum amylase concentration was measured by a colorimetric method after reacting with substrate using the Phadebas amylase test tablet (Magle Life Sciences, Cambridge, MA) and Tecan-infinite M200 Pro plate reader (1).

Myeloperoxidase (MPO) assay. MPO was measured using previously described methods with modifications (1). To calculate the mUnits of MPO/mg of protein the protein concentration of the supernates were measured using the Micro BCA Protein Assay Kit (Thermo Scientific Kit; catalog #23235).

Hematoxylin and Eosin (H&E) staining. In Yoda1-mediated pancreatitis the body region of the pancreas was used for H&E staining (1) and in partial duct ligation mediated pancreatitis the tail region of the pancreas was used. The histological score was calculated from the pathological parameters e.g., tissue edema, neutrophil infiltration, necrosis and hemorrhage with minimum to a severe scoring range of 0-3, 0-3, 0-7 and 0-7, respectively (91). The scores from all parameters were summed to obtain a total histological score.

Real-time PCR. RNAs were isolated using the RiboPure Kit (Invitrogen, catalog #AM1924) followed by DNase1 digestion (Invitrogen; catalog #AM1906) (1).

Statistical analysis. Results were expressed as mean ± SEM. Mean differences between two groups were analyzed by two-tailed Student's *t* test and mean differences between multiple groups were analyzed by one way ANOVA with the Tukey's Multiple

Comparison post-test (GraphPad; prism 8). *P* values <0.05 were considered significant. * $P \leq 0.05$; ** $P \leq 0.01$; *** $P \leq 0.001$, **** $P \leq 0.0001$.

Author contributions: R.A.L ., S.M.S and J.M-J.R designed the experiments. S.M.S ., J.M-J.R and R.A.S performed the experiments and analyzed the data. S.M.S and R.A.L wrote the manuscript. S.J.P. and S.R.V. provided critical review of the data and advice throughout the research. W. L. reviewed the manuscript, offered advice and provided the TRPV4 KO mice. R.A.L. supervised the project and provided funding for the project. All authors reviewed the manuscript.

Acknowledgments:

This work was supported by NIH grants DK064213, DK120555, and the Department of Veterans Affairs. The authors wish to thank Dr. Jorg Grandl for helpful advice and for reviewing the manuscript. We acknowledge the generous assistance of Dr. Yasheng Gao from the Duke University Light Microscopy Core. The authors also acknowledge support from the Duke Comprehensive Cancer Center and the Duke Transgenic Core Facilities.

References

1. Romac JM, Shahid RA, Swain SM, Vigna SR, and Liddle RA. Piezo1 is a mechanically activated ion channel and mediates pressure induced pancreatitis. *Nature Communications.* 2018;9(1):1715.

2. Yamamoto M, Otani M, and Otsuki M. A new model of chronic pancreatitis in rats. *Am J Physiol Gastrointest Liver Physiol.* 2006;291(4):G700-8.

3. Watanabe S, Nagashio Y, Asaumi H, Nomiyama Y, Taguchi M, Tashiro M, et al. Pressure activates rat pancreatic stellate cells. *Am J Physiol Gastrointest Liver Physiol.* 2004;287(6):G1175-81.

4. Opie EL, and Meakins JC. Data Concerning the Etiology and Pathology of Hemorrhagic Necrosis of the Pancreas (Acute Hemorrhagic Pancreatitis). *J Exp Med.* 1909;11(4):561-78.

5. Lerch MM, Saluja AK, Runzi M, Dawra R, Saluja M, and Steer ML. Pancreatic duct obstruction triggers acute necrotizing pancreatitis in the opossum. *Gastroenterology.* 1993;104(3):853-61.

6. Gukovskaya AS, Perkins P, Zaninovic V, Sandoval D, Rutherford R, Fitzsimmons T, et al. Mechanisms of cell death after pancreatic duct obstruction in the opossum and the rat. *Gastroenterology.* 1996;110(3):875-84.

7. van Santvoort HC, Besselink MG, de Vries AC, Boermeester MA, Fischer K, Bollen TL, et al. Early endoscopic retrograde cholangiopancreatography in predicted severe acute biliary pancreatitis: a prospective multicenter study. *Ann Surg.* 2009;250(1):68-75.

8. Committee ASoP, Anderson MA, Fisher L, Jain R, Evans JA, Appalaneni V, et al. Complications of ERCP. *Gastrointest Endosc.* 2012;75(3):467-73.

9. Malgras B, Douard R, Siauve N, and Wind P. Invited Commentary Management of Left Pancreatic Trauma. *American Surgeon.* 2011;77(1):1-9.

10. Coste B, Mathur J, Schmidt M, Earley TJ, Ranade S, Petrus MJ, et al. Piezo1 and Piezo2 are essential components of distinct mechanically activated cation channels. *Science.* 2010;330(6000):55-60.

11. Poole K, Herget R, Lapatsina L, Ngo HD, and Lewin GR. Tuning Piezo ion channels to detect molecular-scale movements relevant for fine touch. *Nat Commun.* 2014;5:3520.

12. Ranade SS, Qiu Z, Woo SH, Hur SS, Murthy SE, Cahalan SM, et al. Piezo1, a mechanically activated ion channel, is required for vascular development in mice. *Proc Natl Acad Sci U S A.* 2014;111(28):10347-52.

13. Wang S, Chennupati R, Kaur H, Iring A, Wettschureck N, and Offermanns S. Endothelial cation channel PIEZO1 controls blood pressure by mediating flow-induced ATP release. *J Clin Invest.* 2016;126(12):4527-36.

14. Syeda R, Florendo MN, Cox CD, Kefauver JM, Santos JS, Martinac B, et al. Piezo1 Channels Are Inherently Mechanosensitive. *Cell Rep.* 2016;17(7):1739-46.

15. Syeda R, Xu J, Dubin AE, Coste B, Mathur J, Huynh T, et al. Chemical activation of the mechanotransduction channel Piezo1. *Elife.* 2015;4.

16. Li J, Hou B, Tumova S, Muraki K, Bruns A, Ludlow MJ, et al. Piezo1 integration of vascular architecture with physiological force. *Nature.* 2014;515(7526):279-82.

17. Miyamoto T, Mochizuki T, Nakagomi H, Kira S, Watanabe M, Takayama Y, et al. Functional role for Piezo1 in stretch-evoked Ca(2)(+) influx and ATP release in urothelial cell cultures. *J Biol Chem.* 2014;289(23):16565-75.

18. Petersen OH, and Ueda N. Pancreatic acinar cells: the role of calcium in stimulus-secretion coupling. *J Physiol.* 1976;254(3):583-606.

19. Williams JA. Regulation of pancreatic acinar cell function by intracellular calcium. *Am J Physiol.* 1980;238(4):G269-79.

20. Gallacher DV, Hanley MR, Petersen OH, Roberts ML, Squire-Pollard LG, and Yule DI. Substance P and bombesin elevate cytosolic Ca2+ by different molecular mechanisms in a rat pancreatic acinar cell line. *J Physiol.* 1990;426:193-207.

21. Iwatsuki N, and Petersen OH. In vitro action of bombesin on amylase secretion, membrane potential, and membrane resistance in rat and mouse pancreatic acinar cells. A comparison with other secretagogues. *J Clin Invest.* 1978;61(1):41-6.

22. Chandra R, and Liddle RA. Regulation of Pancreatic Secretion. *Pancreapedia.* 2015;Versio 1.0:1-40.

23. Gerasimenko JV, Gerasimenko OV, and Petersen OH. The role of Ca2+ in the pathophysiology of pancreatitis. *J Physiol.* 2014;592(2):269-80.

24. Gerasimenko JV, Gryshchenko O, Ferdek PE, Stapleton E, Hebert TO, Bychkova S, et al. Ca2+ release-activated Ca2+ channel blockade as a potential tool in antipancreatitis therapy. *Proc Natl Acad Sci U S A.* 2013;110(32):13186-91.

25. Lerch MM, Halangk W, and Mayerle J. Preventing pancreatitis by protecting the mitochondrial permeability transition pore. *Gastroenterology.* 2013;144(2):265-9.

26. Vonlaufen A, Phillips PA, Xu Z, Zhang X, Yang L, Pirola RC, et al. Withdrawal of alcohol promotes regression while continued alcohol intake promotes persistence of LPS-induced pancreatic injury in alcohol-fed rats. *Gut.* 2011;60(2):238-46.

27. Booth DM, Murphy JA, Mukherjee R, Awais M, Neoptolemos JP, Gerasimenko OV, et al. Reactive oxygen species induced by bile acid induce apoptosis and protect against necrosis in pancreatic acinar cells. *Gastroenterology.* 2011;140(7):2116-25.

28. Huang W, Booth DM, Cane MC, Chvanov M, Javed MA, Elliott VL, et al. Fatty acid ethyl ester synthase inhibition ameliorates ethanol-induced Ca2+-dependent mitochondrial dysfunction and acute pancreatitis. *Gut.* 2014;63(8):1313-24.

29. Shalbueva N, Mareninova OA, Gerloff A, Yuan J, Waldron RT, Pandol SJ, et al. Effects of oxidative alcohol metabolism on the mitochondrial permeability transition pore and

necrosis in a mouse model of alcoholic pancreatitis. *Gastroenterology.* 2013;144(2):437-46 e6.

30. Friedrich EE, Hong Z, Xiong S, Zhong M, Di A, Rehman J, et al. Endothelial cell Piezo1 mediates pressure-induced lung vascular hyperpermeability via disruption of adherens junctions. *Proc Natl Acad Sci U S A.* 2019;116(26):12980-5.

31. Everaerts W, Zhen X, Ghosh D, Vriens J, Gevaert T, Gilbert JP, et al. Inhibition of the cation channel TRPV4 improves bladder function in mice and rats with cyclophosphamide-induced cystitis. *Proc Natl Acad Sci U S A.* 2010;107(44):19084-9.

32. Sonkusare SK, Bonev AD, Ledoux J, Liedtke W, Kotlikoff MI, Heppner TJ, et al. Elementary Ca2+ signals through endothelial TRPV4 channels regulate vascular function. *Science.* 2012;336(6081):597-601.

33. Thorneloe KS, Cheung M, Bao W, Alsaid H, Lenhard S, Jian MY, et al. An orally active TRPV4 channel blocker prevents and resolves pulmonary edema induced by heart failure. *Sci Transl Med.* 2012;4(159):159ra48.

34. Mochizuki T, Sokabe T, Araki I, Fujishita K, Shibasaki K, Uchida K, et al. The TRPV4 cation channel mediates stretch-evoked Ca2+ influx and ATP release in primary urothelial cell cultures. *J Biol Chem.* 2009;284(32):21257-64.

35. Pochynyuk O, Zaika O, O'Neil RG, and Mamenko M. Novel insights into TRPV4 function in the kidney. *Pflugers Arch.* 2013;465(2):177-86.

36. Vergnolle N, Cenac N, Altier C, Cellars L, Chapman K, Zamponi GW, et al. A role for transient receptor potential vanilloid 4 in tonicity-induced neurogenic inflammation. *Br J Pharmacol.* 2010;159(5):1161-73.

37. Andrade YN, Fernandes J, Vazquez E, Fernandez-Fernandez JM, Arniges M, Sanchez TM, et al. TRPV4 channel is involved in the coupling of fluid viscosity changes to epithelial ciliary activity. *J Cell Biol.* 2005;168(6):869-74.

38. Alessandri-Haber N, Dina OA, Chen X, and Levine JD. TRPC1 and TRPC6 channels cooperate with TRPV4 to mediate mechanical hyperalgesia and nociceptor sensitization. *J Neurosci.* 2009;29(19):6217-28.

39. Rahaman SO, Grove LM, Paruchuri S, Southern BD, Abraham S, Niese KA, et al. TRPV4 mediates myofibroblast differentiation and pulmonary fibrosis in mice. *J Clin Invest.* 2014;124(12):5225-38.

40. Hof T, Chaigne S, Recalde A, Salle L, Brette F, and Guinamard R. Transient receptor potential channels in cardiac health and disease. *Nat Rev Cardiol.* 2019;16(6):344-60.

41. Ranade SS, Syeda R, and Patapoutian A. Mechanically Activated Ion Channels. *Neuron.* 2015;87(6):1162-79.

42. Vriens J, Watanabe H, Janssens A, Droogmans G, Voets T, and Nilius B. Cell swelling, heat, and chemical agonists use distinct pathways for the activation of the cation channel TRPV4. *Proceedings of the National Academy of Sciences.* 2004;101(1):396-401.

43. Watanabe H, Vriens J, Prenen J, Droogmans G, Voets T, and Nilius B. Anandamide and arachidonic acid use epoxyeicosatrienoic acids to activate TRPV4 channels. *Nature.* 2003;424(6947):434-8.

44. Fan HC, Zhang X, and McNaughton PA. Activation of the TRPV4 ion channel is enhanced by phosphorylation. *J Biol Chem.* 2009;284(41):27884-91.

45. Cao S, Anishkin A, Zinkevich NS, Nishijima Y, Korishettar A, Wang Z, et al. Transient receptor potential vanilloid 4 (TRPV4) activation by arachidonic acid requires protein kinase A-mediated phosphorylation. *J Biol Chem.* 2018;293(14):5307-22.

46. Bae C, Sachs F, and Gottlieb PA. The mechanosensitive ion channel Piezo1 is inhibited by the peptide GsMTx4. *Biochemistry.* 2011;50(29):6295-300.

47. Nathan JD, Romac J, Peng RY, Peyton M, Macdonald RJ, and Liddle RA. Transgenic expression of pancreatic secretory trypsin inhibitor-I ameliorates secretagogue-induced pancreatitis in mice. *Gastroenterology.* 2005;128(3):717-27.

48. Gukovskaya AS, Gukovsky I, Jung Y, Mouria M, and Pandol SJ. Cholecystokinin induces caspase activation and mitochondrial dysfunction in pancreatic acinar cells. Roles in cell injury processes of pancreatitis. *J Biol Chem.* 2002;277(25):22595-604.

49. Lugea A, Waldron RT, Mareninova OA, Shalbueva N, Deng N, Su HY, et al. Human Pancreatic Acinar Cells: Proteomic Characterization, Physiologic Responses, and Organellar Disorders in ex Vivo Pancreatitis. *Am J Pathol.* 2017;187(12):2726-43.

50. Pandol SJ, Schoeffield MS, Sachs G, and Muallem S. Role of free cytosolic calcium in secretagogue-stimulated amylase release from dispersed acini from guinea pig pancreas. *J Biol Chem.* 1985;260(18):10081-6.

51. Pandol SJ, Schoeffield MS, Fimmel CJ, and Muallem S. The agonist-sensitive calcium pool in the pancreatic acinar cell. Activation of plasma membrane Ca2+ influx mechanism. *J Biol Chem.* 1987;262(35):16963-8.

52. Raraty M, Ward J, Erdemli G, Vaillant C, Neoptolemos JP, Sutton R, et al. Calcium-dependent enzyme activation and vacuole formation in the apical granular region of pancreatic acinar cells. *Proc Natl Acad Sci U S A.* 2000;97(24):13126-31.

53. Walsh DWM, Siebenwirth C, Greubel C, Ilicic K, Reindl J, Girst S, et al. Live cell imaging of mitochondria following targeted irradiation in situ reveals rapid and highly localized loss of membrane potential. *Sci Rep.* 2017;7:46684.

54. Lerch MM, and Gorelick FS. Early trypsinogen activation in acute pancreatitis. *Med Clin North Am.* 2000;84(3):549-63, viii.

55. Gerasimenko JV, Lur G, Ferdek P, Sherwood MW, Ebisui E, Tepikin AV, et al. Calmodulin protects against alcohol-induced pancreatic trypsinogen activation elicited via Ca2+ release through IP3 receptors. *Proc Natl Acad Sci U S A.* 2011;108(14):5873-8.

56. Halestrap AP, and Richardson AP. The mitochondrial permeability transition: a current perspective on its identity and role in ischaemia/reperfusion injury. *J Mol Cell Cardiol.* 2015;78:129-41.

57. Bagher P, Beleznai T, Kansui Y, Mitchell R, Garland CJ, and Dora KA. Low intravascular pressure activates endothelial cell TRPV4 channels, local Ca2+ events, and IKCa channels, reducing arteriolar tone. *Proc Natl Acad Sci U S A.* 2012;109(44):18174-9.

58. Hamaguchi K, Kuwata H, Yoshihara K, Masuda S, Shimbara S, Oh-ishi S, et al. Induction of distinct sets of secretory phospholipase A(2) in rodents during inflammation. *Biochim Biophys Acta.* 2003;1635(1):37-47.

59. Riendeau D, Guay J, Weech PK, Laliberte F, Yergey J, Li C, et al. Arachidonyl trifluoromethyl ketone, a potent inhibitor of 85-kDa phospholipase A2, blocks production of arachidonate and 12-hydroxyeicosatetraenoic acid by calcium ionophore-challenged platelets. *J Biol Chem.* 1994;269(22):15619-24.

60. Criddle DN, Gerasimenko JV, Baumgartner HK, Jaffar M, Voronina S, Sutton R, et al. Calcium signalling and pancreatic cell death: apoptosis or necrosis? *Cell Death Differ.* 2007;14(7):1285-94.

61. Acosta JM, and Ledesma CL. Gallstone migration as a cause of acute pancreatitis. *N Engl J Med.* 1974;290(9):484-7.

62. Neoptolemos JP, Carr-Locke DL, London N, Bailey I, and Fossard DP. ERCP findings and the role of endoscopic sphincterotomy in acute gallstone pancreatitis. *Br J Surg.* 1988;75(10):954-60.

63. Bradley EL, 3rd. Pancreatic duct pressure in chronic pancreatitis. *Am J Surg.* 1982;144(3):313-6.

64. Alper SL. Genetic Diseases of PIEZO1 and PIEZO2 Dysfunction. *Curr Top Membr.* 2017;79:97-134.

65. Lewis AH, Cui AF, McDonald MF, and Grandl J. Transduction of Repetitive Mechanical Stimuli by Piezo1 and Piezo2 Ion Channels. *Cell Rep.* 2017;19(12):2572-85.

66. Petersen OH. Ca2+-induced pancreatic cell death: roles of the endoplasmic reticulum, zymogen granules, lysosomes and endosomes. *J Gastroenterol Hepatol.* 2008;23 Suppl 1:S31-6.

67. Li J, Zhou R, Zhang J, and Li ZF. Calcium signaling of pancreatic acinar cells in the pathogenesis of pancreatitis. *World J Gastroenterol.* 2014;20(43):16146-52.

68. Petersen OH, and Tepikin AV. Polarized calcium signaling in exocrine gland cells. *Annu Rev Physiol.* 2008;70:273-99.

69. Voronina SG, Gryshchenko OV, Gerasimenko OV, Green AK, Petersen OH, and Tepikin AV. Bile acids induce a cationic current, depolarizing pancreatic acinar cells and increasing the intracellular Na+ concentration. *J Biol Chem.* 2005;280(3):1764-70.

70. Pandol SJ, Saluja AK, Imrie CW, and Banks PA. Acute pancreatitis: bench to the bedside. *Gastroenterology.* 2007;132(3):1127-51.

71. Criddle DN, Murphy J, Fistetto G, Barrow S, Tepikin AV, Neoptolemos JP, et al. Fatty acid ethyl esters cause pancreatic calcium toxicity via inositol trisphosphate receptors and loss of ATP synthesis. *Gastroenterology.* 2006;130(3):781-93.

72. Leach SD, Modlin IM, Scheele GA, and Gorelick FS. Intracellular activation of digestive zymogens in rat pancreatic acini. Stimulation by high doses of cholecystokinin. *J Clin Invest.* 1991;87(1):362-6.

73. Criddle DN, McLaughlin E, Murphy JA, Petersen OH, and Sutton R. The pancreas misled: signals to pancreatitis. *Pancreatology.* 2007;7(5-6):436-46.

74. Mukherjee R, Mareninova OA, Odinokova IV, Huang W, Murphy J, Chvanov M, et al. Mechanism of mitochondrial permeability transition pore induction and damage in the pancreas: inhibition prevents acute pancreatitis by protecting production of ATP. *Gut.* 2016;65(8):1333-46.

75. Alavian KN, Beutner G, Lazrove E, Sacchetti S, Park HA, Licznerski P, et al. An uncoupling channel within the c-subunit ring of the F1FO ATP synthase is the mitochondrial permeability transition pore. *Proc Natl Acad Sci U S A.* 2014;111(29):10580-5.

76. Giorgio V, von Stockum S, Antoniel M, Fabbro A, Fogolari F, Forte M, et al. Dimers of mitochondrial ATP synthase form the permeability transition pore. *Proc Natl Acad Sci U S A.* 2013;110(15):5887-92.

77. Elrod JW, Wong R, Mishra S, Vagnozzi RJ, Sakthievel B, Goonasekera SA, et al. Cyclophilin D controls mitochondrial pore-dependent Ca(2+) exchange, metabolic flexibility, and propensity for heart failure in mice. *J Clin Invest.* 2010;120(10):3680-7.

78. Saluja AK, Bhagat L, Lee HS, Bhatia M, Frossard JL, and Steer ML. Secretagogue-induced digestive enzyme activation and cell injury in rat pancreatic acini. *Am J Physiol.* 1999;276(4 Pt 1):G835-42.

79. Mooren F, Hlouschek V, Finkes T, Turi S, Weber IA, Singh J, et al. Early changes in pancreatic acinar cell calcium signaling after pancreatic duct obstruction. *J Biol Chem.* 2003;278(11):9361-9.

80. Watanabe H, Vriens J, Suh SH, Benham CD, Droogmans G, and Nilius B. Heat-evoked activation of TRPV4 channels in a HEK293 cell expression system and in native mouse aorta endothelial cells. *J Biol Chem.* 2002;277(49):47044-51.

81. Yule DI. Ca2+ Signaling in Pancreatic Acinar Cells. *Pancreapedia.* 2015(Version 1.0).

82. Cosen-Binker LI, and Gaisano HY. Recent insights into the cellular mechanisms of acute pancreatitis. *Can J Gastroenterol.* 2007;21(1):19-24.

83. Sendler M, Weiss FU, Golchert J, Homuth G, van den Brandt C, Mahajan UM, et al. Cathepsin B-Mediated Activation of Trypsinogen in Endocytosing Macrophages Increases Severity of Pancreatitis in Mice. *Gastroenterology.* 2018;154(3):704-18.e10.

84. Cahalan SM, Lukacs V, Ranade SS, Chien S, Bandell M, and Patapoutian A. Piezo1 links mechanical forces to red blood cell volume. *Elife.* 2015;4.

85. Kanju P, Chen Y, Lee W, Yeo M, Lee SH, Romac J, et al. Small molecule dual-inhibitors of TRPV4 and TRPA1 for attenuation of inflammation and pain. *Sci Rep.* 2016;6:26894.

86. Liddle RA, Goldfine ID, and Williams JA. Bioassay of plasma cholecystokinin in rats: effects of food, trypsin inhibitor, and alcohol. *Gastroenterology.* 1984;87(3):542-9.

87. Williams JA. Isolation of rodent pancreatic acinar cells and acini by collagenase digestion. *Pancreapedia.* 2010;Exocrine Pancreas Knowledge Base.

88. Li J, Tan H, Wang X, Li Y, Samuelson L, Li X, et al. Circulating fibrocytes stabilize blood vessels during angiogenesis in a paracrine manner. *The American journal of pathology.* 2014;184(2):556-71.

89. De Groef S, Leuckx G, Van Gassen N, Staels W, Cai Y, Yuchi Y, et al. Surgical Injury to the Mouse Pancreas through Ligation of the Pancreatic Duct as a Model for Endocrine and Exocrine Reprogramming and Proliferation. *J Vis Exp.* 2015(102):e52765.

90. Sendler M, Beyer G, Mahajan UM, Kauschke V, Maertin S, Schurmann C, et al. Complement Component 5 Mediates Development of Fibrosis, via Activation of Stellate Cells, in 2 Mouse Models of Chronic Pancreatitis. *Gastroenterology.* 2015;149(3):765-76 e10.

91. Spormann H, Sokolowski A, and Letko G. Effect of Temporary Ischemia Upon Development and Histological Patterns of Acute-Pancreatitis in the Rat. *Pathol Res Pract.* 1989;184(5):507-13.

Figures and legends

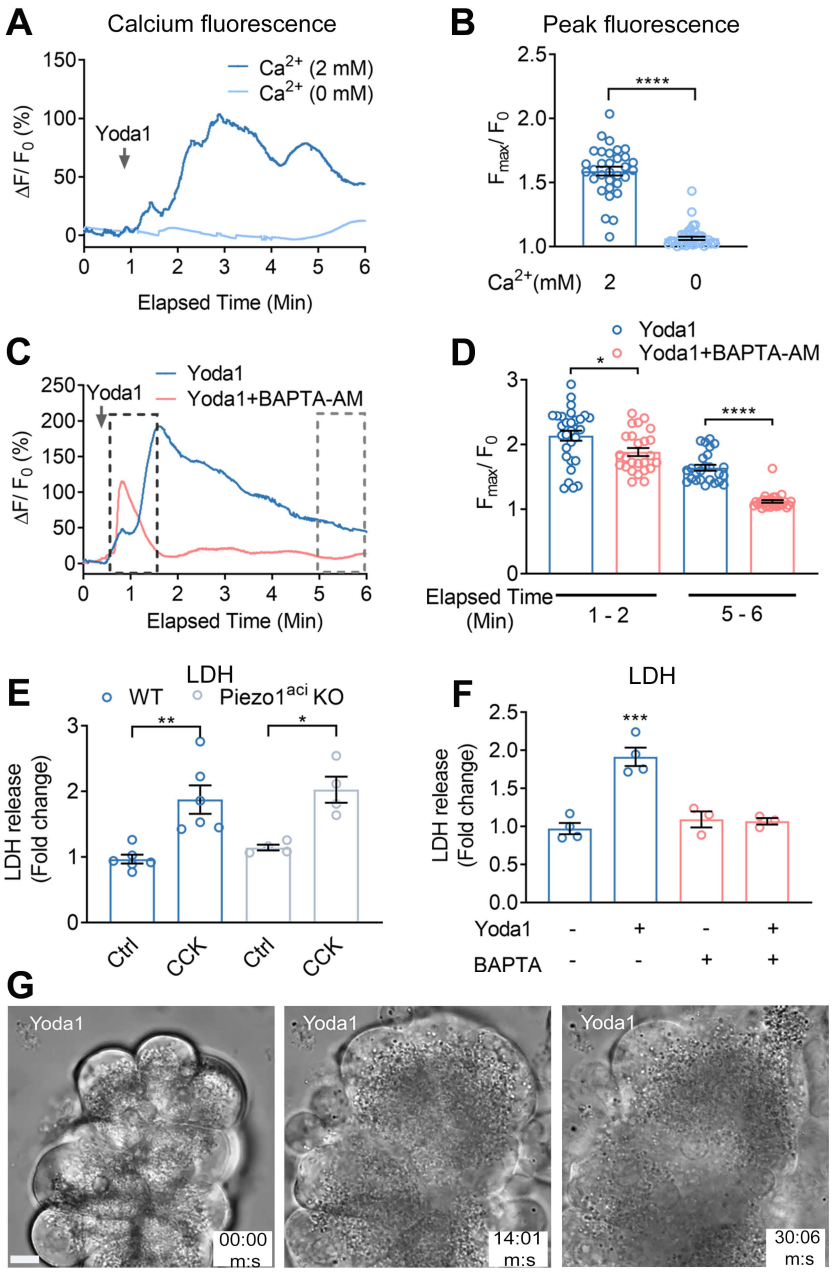

Figure 1. Piezo1 activation increases $[Ca^{2+}]_i$ and induces cell death in pancreatic acini. (A) Live-cell imaging of pancreatic acini loaded with Calcium 6-QF. Pancreatic acini were incubated with Yoda1 (25 μM) in the presence (2 mM) or absence (0 mM) of extracellular calcium. Yoda1 was added at the time indicated by the arrow. (B) Comparison of the Yoda1-induced peak $[Ca^{2+}]_i$ is expressed as the ratio of peak intensity (F_{max})/baseline intensity (F_0) from 32-41 cells. (C) The effects of Yoda1 (50 μM) on $[Ca^{2+}]_i$ in the absence or presence of the calcium chelator BAPTA-AM (20 μM). (D) Statistical analysis of peak (F_{max}/ F_0) from 25-30 cells in which acinar cells were pre-incubated 30 minutes with BAPTA-AM (20 μM) before Yoda1 application. (F_{max}/ F_0) were calculated from the time periods 1-2 minutes and 5-6 minutes to assess the initial transient and sustained $[Ca^{2+}]_i$ levels, respectively. (E) The effects of CCK (1 nM) on LDH release from isolated pancreatic acini from wild type (WT) and Piezo1^{aci} KO mice from 4-6 experiments. (F) The effects of Yoda1 (50 μM) on LDH release from acinar cells with and without pre-incubation of BAPTA-AM for 30 minutes are shown from 3-5 experiments. (G) Bright field images of pancreatic acini at different time points in the presence of Yoda1 (50 μM). Images represent a plane (5 μM thick) from a Z stack of captured images to visualize the changes in cell morphology and granule movement. Images were captured with a 100x oil objective. Statistical analyses: Student's t-test (B, D) and one-way ANOVA with the Tukey's multiple comparison (E and F); $^*P \leq 0.05$; $^{**}P \leq 0.01$; $^{***}P \leq 0.0001$, $^{****}P \leq 0.0001$. Results are expressed as the mean±SEM. Scale bar = 10 μm.

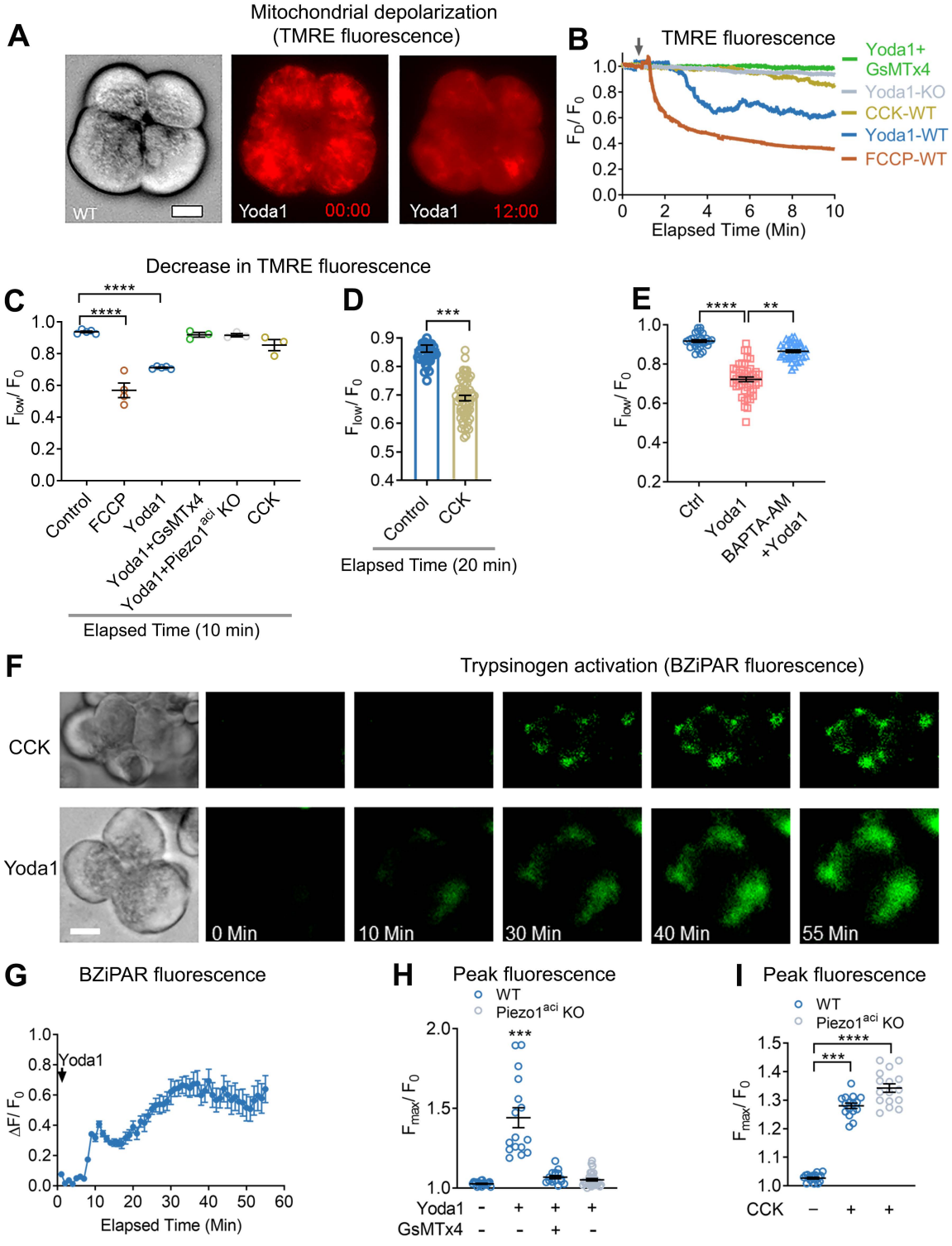

Figure 2. Piezo1 activation induces mitochondrial depolarization and trypsinogen activation in pancreatic acini. (A) Brightfield and fluorescence images of TMRE-loaded pancreatic acini 0 and 12 minutes after Yoda1 (50 μM) application. (B) Traces of live cell TMRE fluorescence intensity of single acinar cells over time following the administration of Yoda1 (arrow). F_D is the decrease in TMRE fluorescence and F_0 is the baseline TMRE intensity. Acini from WT or Piezo1^{aci} KO mice were treated with the mitochondrial uncoupler FCCP (10 μM), Yoda1 (50 μM), Yoda1 + GsMTx4 (5 μM), or CCK (10 nM). A representative tracing from three experiments is shown. (C) The mean decrease in TMRE intensity from panel B is depicted (n=3-5 independent experiments with 15-20 cells in each experiment). (D) A decrease in TMRE intensity of pancreatic acini is shown in response to CCK (10 nM) from 60 cells over 20 minutes. (E) Decrease in fluorescence intensity of TMRE in pancreatic acinar cells upon Yoda1 application with or without preincubation of BAPTA-AM (20 μM) for 20 minutes is shown from 29-45 cells.

(F) Live cell imaging of intracellular trypsin activation with CCK (10 nM) and Yoda1 (50 μM) treatments. (G) The time course of Yoda1-induced trypsin activation is shown for three experiments. (H) Peak BZiPAR fluorescence was measured in acini from WT mice treated with Yoda1 in the absence or presence of GsMTx4 (5 μM) or in acini from Piezo1^{aci} KO mice (n = 3-5 independent experiments with 16-31 cells). (I) Pancreatic acini from Piezo1^{aci} KO mice had a trypsin activation response to CCK (10 nM) similar to wild type mice (n = 3, from 16-20 cells). Statistical analyses: Student's *t*- test (D) and one-way ANOVA (C, E, H and I); mean ± SEM; $^{**}P \leq 0.01$, $^{***}P \leq 0.001$, $^{****}P \leq 0.0001$. Bar = 10 μm.

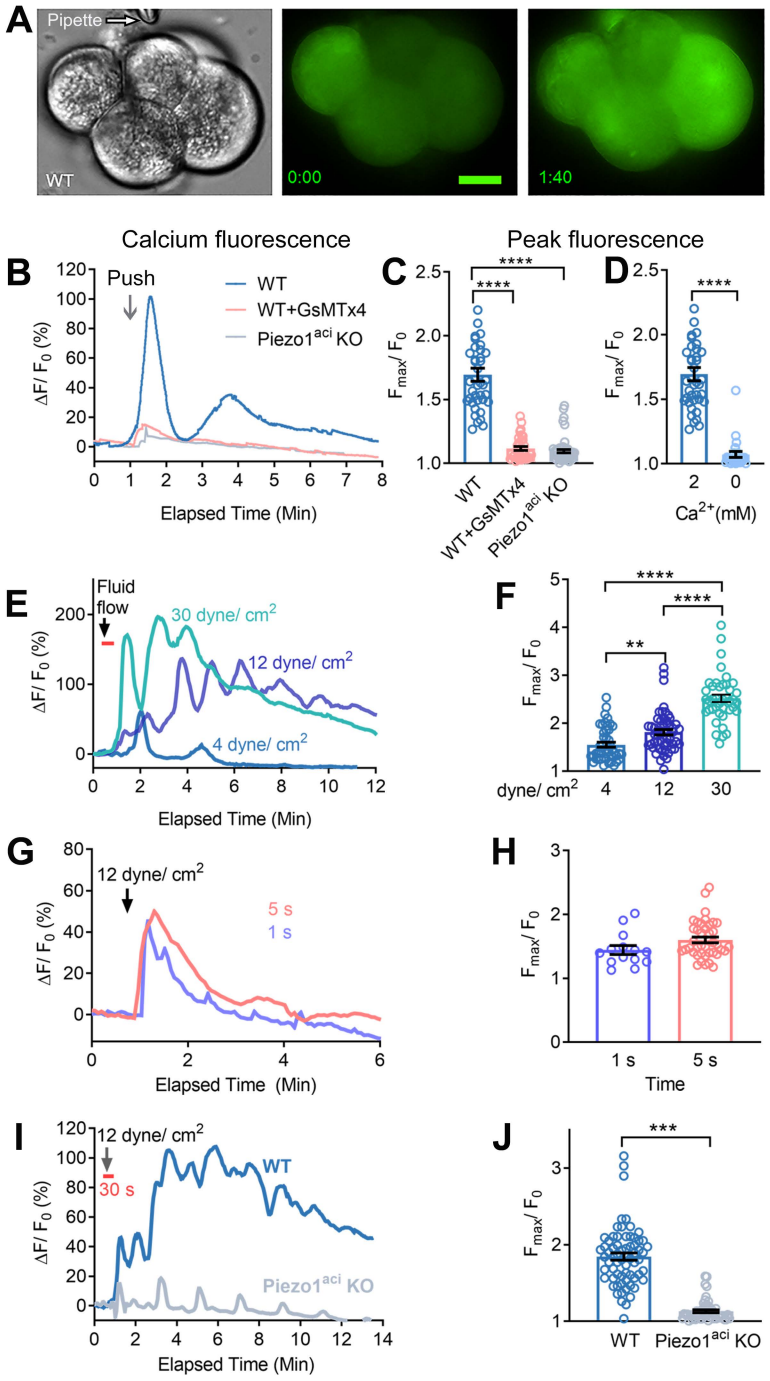

Figure 3. Mechanical pushing and fluid shear stress increases $[Ca^{2+}]_i$ in pancreatic acini. (A) Bright field and live-cell imaging of pancreatic acini loaded with Calcium 6-QF at time 0 and at the time of maximum fluorescence 1:40 (min:sec) after mechanical pushing. (B) Representative $[Ca^{2+}]_i$ fluorescence tracings from single acinar cells in an acinus during the course of mechanical pushing with a blunt pipette. (C) Peak $[Ca^{2+}]_i$ levels following mechanical pushing of acini from wild type or Piezo1^{aci} KO mice. (D) Blunt pushing with a micropipette increased $[Ca^{2+}]_i$ fluorescence only in the presence of extracellular Ca^{2+}. Results represent data from 25-39 cells in 3 independent experiments. (E) Representative traces for relative fluorescence intensity ($\Delta F/F_0$) of Calcium 6-QF-loaded cells are shown in response to applied shear stress at the forces shown in the graph. The duration of fluid flow shear stress was 30 seconds as indicated by the orange bar. (F) The average peak $[Ca^{2+}]_i$ intensity of F_{max}/F_0 is shown for 41-54 cells; n = 3-4 independent experiments. (G and H) The relative fluorescence intensity ($\Delta F/F_0$) and average peak $[Ca^{2+}]_i$ intensity of pancreatic acini in response to 12 dyne/cm^2 shear stress for 1 or 5 seconds. Data in H are averaged from 14-41 cells. (I) Representative traces of relative fluorescence intensity ($\Delta F/F_0$) from Calcium 6-QF loaded wild type and Piezo1 KO acinar cells before and after applying 12 dyne/cm^2 shear stress for 30 seconds. (J) Average peak intensity of F_{max}/F_0 from the experiment depicted in panel I. Data represent a total 53-67 cells and 3 independent experiments. Statistical analyses: Student's t-test (D, H, J) and one-way ANOVA with the Tukey's multiple comparison (C and F); mean±SEM; $^{**}P \leq 0.01$, $^{***}P \leq 0.001$, $^{****}P \leq 0.0001$. Scale bar = 10 μm.

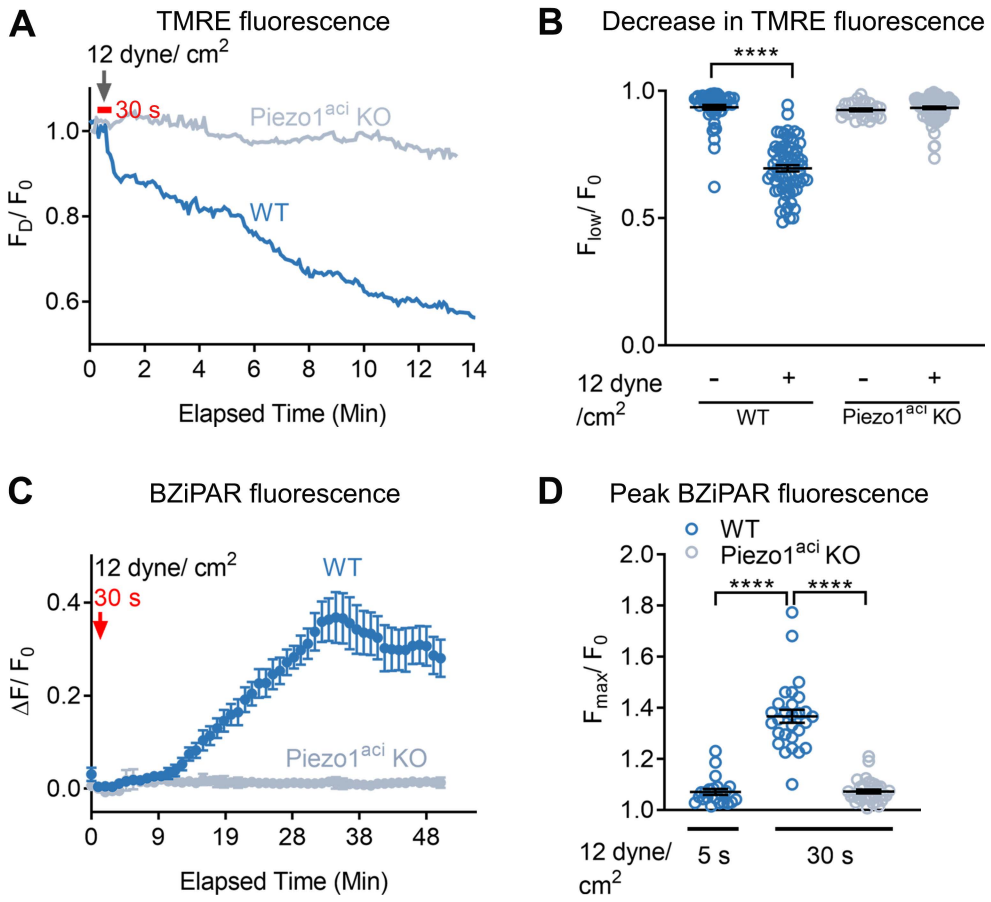

Figure 4. Fluid shear stress induces mitochondrial depolarization and trypsinogen activation in pancreatic acini. (A) Pancreatic acini were subjected to fluid shear force of 12 dyne/cm^2 and TMRE dye fluorescence intensity of pancreatic acinar cells from wild type (WT) and Piezo1^{aci} KO mice were measured over 15 minutes. The duration of shear stress for 30 seconds is marked by the orange bar. F_D is the decrease in TMRE fluorescence over time and F_0 is the base line TMRE intensity before fluid shear stress. (B) The mean average decrease in fluorescence intensity of TMRE over 15 minutes is shown. F_{low} is the lowest TMRE fluorescent intensity after fluid shear stress during imaging. The total number of acinar cells examined: control (without fluid shear stress) = 56; fluid shear stress on wild type acini = 50; and fluid shear stress on Piezo1^{aci} KO acini = 91 and WT acini = 67; n= 3 independent experiments. (C) Traces represent live cell trypsin activity upon fluid shear stress of 12 dyne/cm^2 for 30 seconds in acini from wild type or Piezo1^{aci} KO mice; n=3 experiments. (D) Peak fluorescence intensity of BZiPAR over 50 minutes from 3 experiments; total number of acinar cells were: wild type = 28 and Piezo1^{aci} KO = 36. Values are expressed as the mean ±SEM. ****$P \leq 0.0001$. Statistical analyses were performed using Student's t-test (B) and one-way ANOVA with the Tukey's multiple comparison (D). Scale bar = 10 μm.

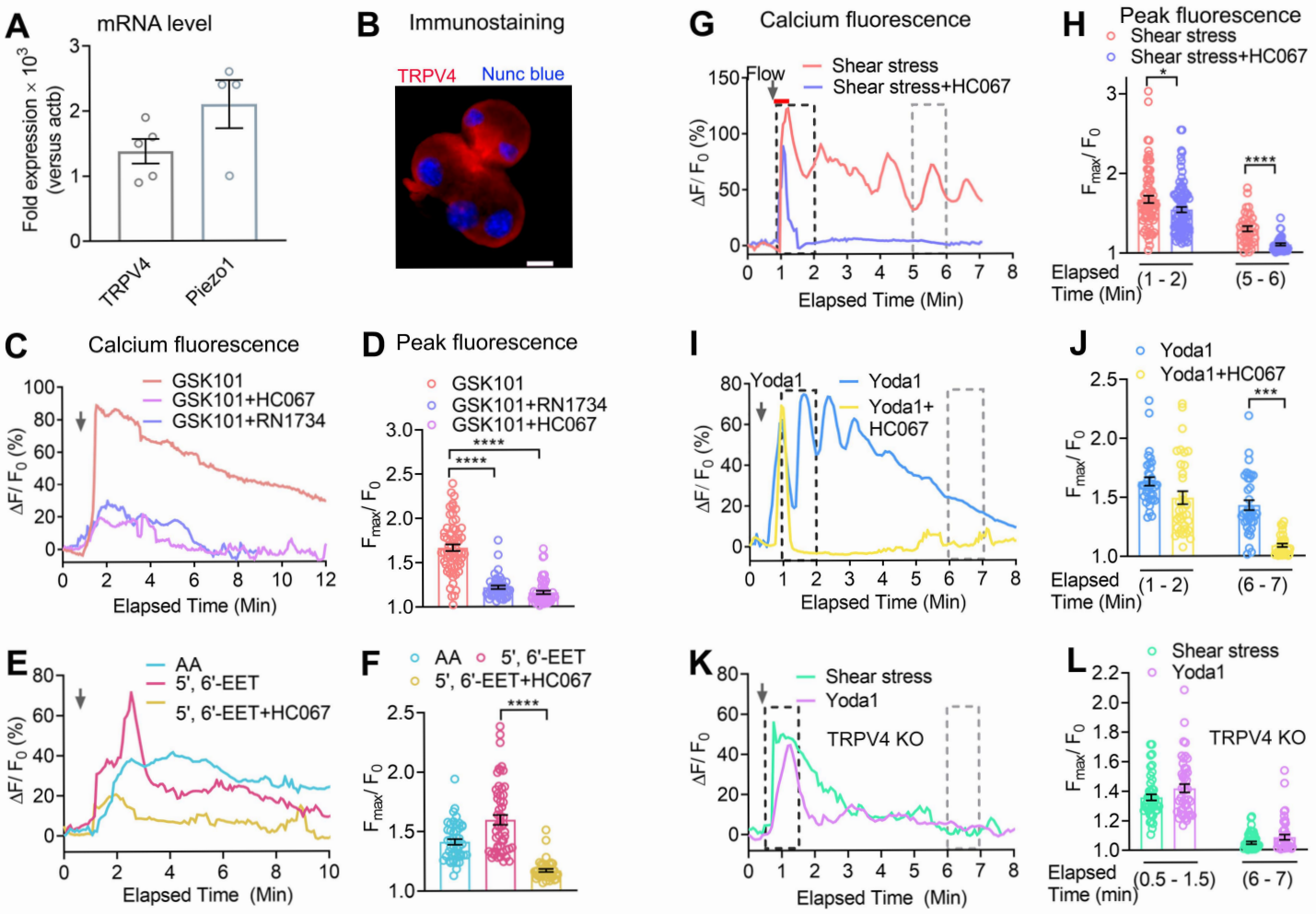

Figure 5. TRPV4 is expressed in pancreatic acini and Piezo1 induces TRPV4 activation. (A) mRNA (fold expression) of TRPV4 and Piezo1 in pancreatic acini relative to the housekeeping gene actb (n= 3-5 experiments). (B) Immunostaining of mouse pancreatic acini with a TRPV4 antibody (red). Nuclei (blue) were stained with Nunc blue. Scale bar = 10 μm. (C and D) Effects of the TRPV4 agonist GSK101 (50 nM) and GSK101 + the TRPV4 antagonist HC067 (100 nM) or RN1734 (30 μM) on $[Ca^{2+}]_i$ are shown. (C) A representative experiment shows the relative fluorescence intensity ($\Delta F/F_0$) of calcium dye over time and (D) is the average peak $[Ca^{2+}]_i$ intensity of pancreatic acini from 43 - 63 cells. (E and F) Arachidonic acid (20 μM) and 5', 6'- eicosatrienoic acid (5 μM) increased $[Ca^{2+}]_i$. The effects of 5', 6'- eicosatrienoic acid (5',6' EET) (5 μM) were blocked by HC067 (100 nM). (E) The relative fluorescence intensity of calcium dye and (F) average peak $[Ca^{2+}]_i$ intensity of pancreatic acini from 40-54 cells are shown. (G, H, I, J) The TRPV4 antagonist HC067 (1 μM) blocked the effects of shear stress (12 dyne/cm^2) and Yoda1 (25 μM) on the sustained $[Ca^{2+}]_i$ responses. (G and I) Representative tracings of the relative fluorescence intensity of calcium dye over time with the different stimuli. (H and J) The average peak $[Ca^{2+}]_i$ responses were calculated from 35-86 cells. (K and L) The shear stress- and Yoda- induced sustained increases in $[Ca^{2+}]_i$ were not seen in pancreatic acini isolated from TRPV4 KO mice. (K) Representative traces demonstrate the effects of shear stress or Yoda1 on $[Ca^{2+}]_i$ and (L) shows the average peak $[Ca^{2+}]_i$ intensity at different time intervals (from 45-47 cells). Statistical analyses were performed using Student's t-test. Values are expressed as the mean ±SEM. *$P \leq 0.05$,***$P \leq 0.001$; ****$P \leq 0.0001$. Scale bar = 10 μm.

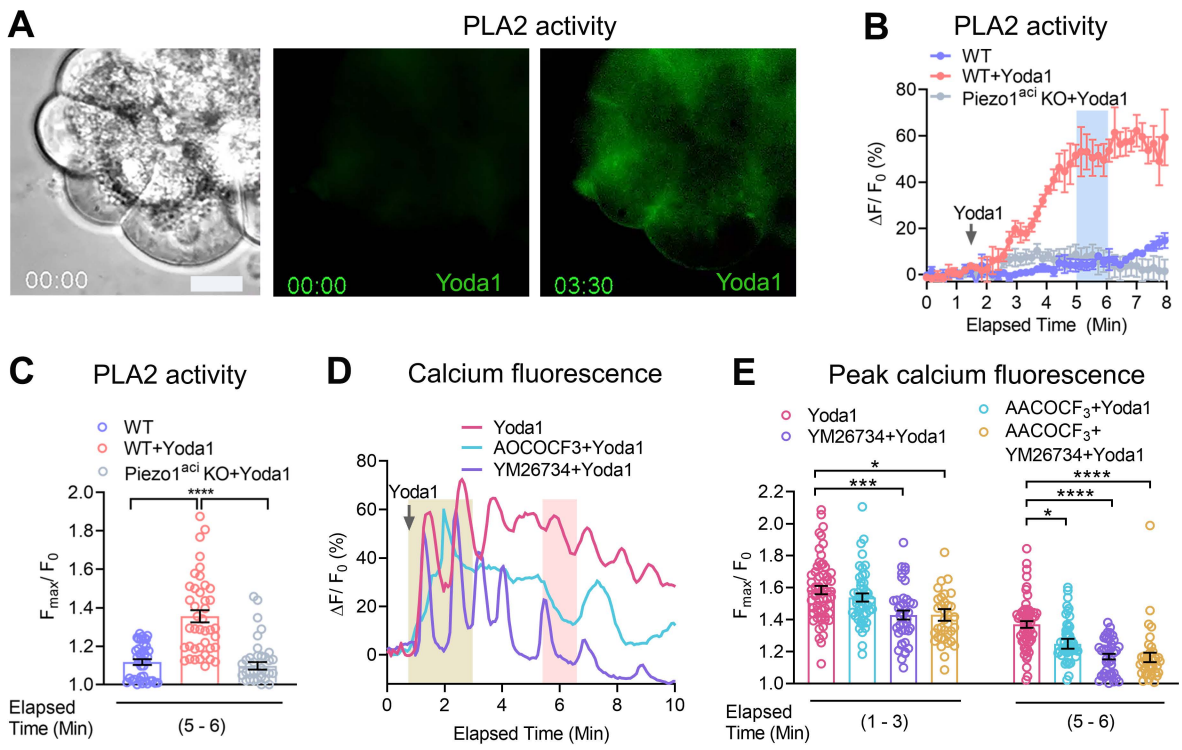

Figure 6. The Piezo1 agonist, Yoda1, induces activation of phospholipase A2 activity.
(A) Brightfield and fluorescence images of BODIPY™ FL C11-PC loaded pancreatic acini at time 0 and 3:30 minutes after Yoda1 (25 μM) application. Scale bar = 10 μm. (B) Traces represent the live cell PLA2 activity upon Yoda1 (25 M) application from four experiments. Representative tracings of acini from wild type and Piezo1aci KO mice are shown. The peak fluorescence intensity was calculated from the elapsed time at 5-6 minutes (blue bar). (C) Peak fluorescence intensity of BODIPY™ FL C11-PC dye measured at an elapsed time of 5-6 minutes from 40-51 cells. (D and E) The traces and graph show the effects of Yoda1 (25 μM) on $[Ca^{2+}]_i$ in pancreatic acini with or without treatment with the cytoplasmic PLA2 blocker AACOCF3 (30 μM) and secretory PLA2 blocker YM26734 (10 μM). YM26734 and AACOCF3 were pre-incubated 10 minutes before application of Yoda1. The transient calcium peaks were measured from signals obtained between 1 to 3 minutes (yellow bar) and sustained calcium peaks were measured from signals between 5.5 to 6.5 minutes (pink bar). Data represent the averages of 36-58 cells. Values were expressed as the means±SEM and mean differences between multiple groups were analyzed by one-way ANOVA with the Tukey's multiple comparison. P values <0.05 were considered significant. *$P \leq 0.05$; *** $P \leq 0.001$; ****$P \leq 0.0001$.

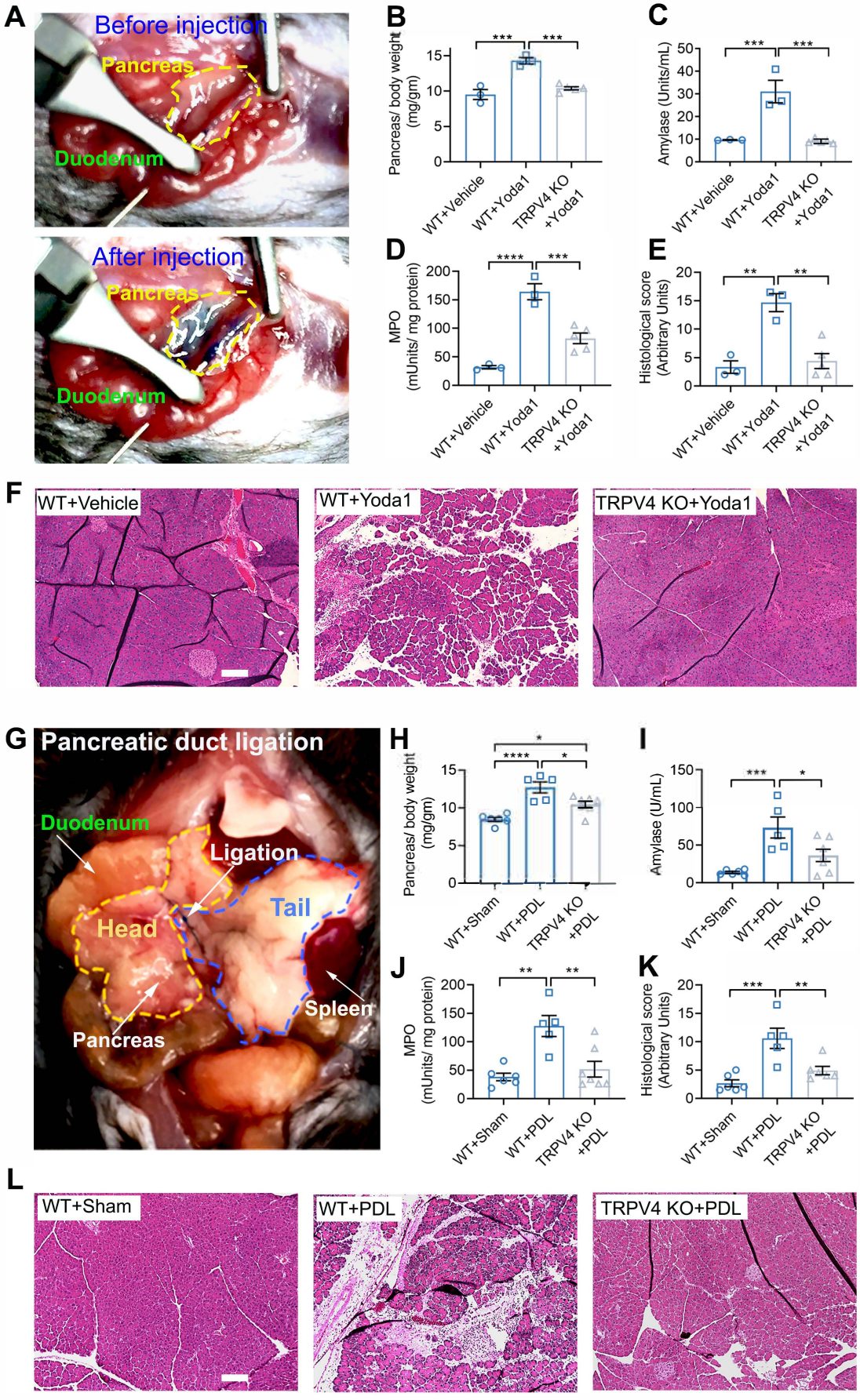

Figure 7. TRPV4 knockout mice are protected against Yodal- and pancreatic pressure induced-pancreatitis. (A) A photograph of the surgical approach used for injection of Yodal into the pancreatic

Methylene blue dye was mixed with the injected solution to aid with pancreatic duct visualization. A total of 50 μL were injected over 10 minutes. The amount of Yoda1 injected into the pancreatic duct was 0.4 mg/kg. The boundary of the mouse pancreas is marked with yellow before and after Yoda1 infusion. After injection methylene blue in the solution made the pancreas blue in color. Pancreatitis parameters included edema (B), serum amylase (C), tissue MPO (D), and pancreatic histology score (E) in vehicle- and Yoda1-treated wild type (WT) and TRPV4 KO mice (n = 3-5). (F) Representative H&E stained images of the mid-region of pancreas are shown (scale bar = 100 μm). (G) A photograph of the partial pancreatic duct ligation (PDL) procedure is shown. The head and tail regions of pancreas are outlined in yellow and blue, respectively. PDL-induced pancreatitis parameters included edema (H), serum amylase (I), pancreatic MPO (J), and pancreas histology scores (K) of the sham and PDL wild type and TRPV4 KO mice (n = 5-7). (L) Representative H&E images of the mid-region of the pancreas are shown (scale bar = 100 μm). Statistical analyses were performed using one-way ANOVA with the Tukey's multiple comparison. Values represent the mean ±SEM; $^{*}P \leq 0.05$, $^{**}P \leq 0.01$, $^{***}P \leq 0.001$, $^{****}P \leq 0.0001$.